International Magnetic Measurement Workshop 21

ESRF, Grenoble, FR, June 2019

A stretched wire system for the measurement of accelerator lattice and insertion device magnets

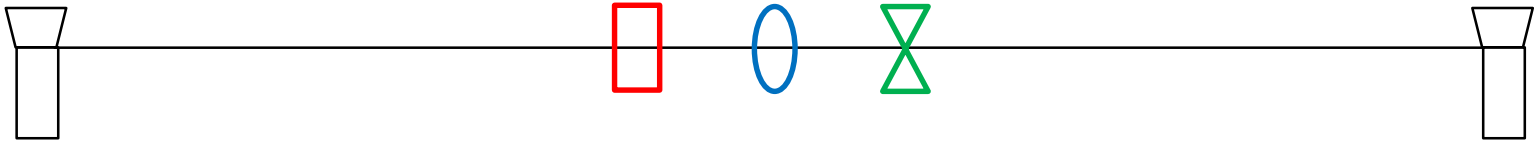

Cheng Ying Kuo, J-C Jan, F-Y Lin, C-K Yang, T-Y Chung, Ching Shiang Hwang

National Synchrotron Radiation Research Center (NSRRC)

Hsinchu, Taiwan

Contents

- Motivation
- Analysis Method and Simulation Results
- Stretched wire measurement system
- Experimental results
  - A Quadrupole Magnet
  - In-vacuum Undulator
  - Circular path
  - Elliptical path
- Conclusions

Introduction

TLS: Taiwan Light Source (1993-now)
TPS: Taiwan Photon Source (2015-now)

2014	Aug.	Booster ring and storage ring accelerators installed
	Dec.	The first TPS light at the 3-GeV design beam energy delivered.
2015	Jan.	Taiwan Photon Source Inauguration Ceremony.
	Dec.	TPS exceeds its design beam current 500 mA
2016	Sep.	TPS Opening Ceremony. Four TPS phase-I beamlines available to users worldwide.
2017	May.	Flagship Project initiated – construction of 5 TPS phase-II beamlines begins
	Dec.	Construction of TPS phase-I beamlines completed

Motivation

- Small bore measurement for ultimate storage ring.
- Elliptical measurement for closed aperture of dipole and insertion device.

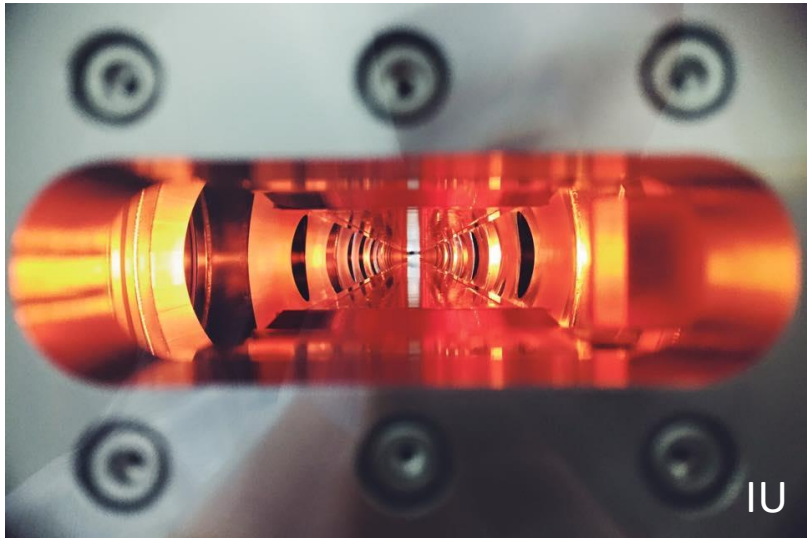

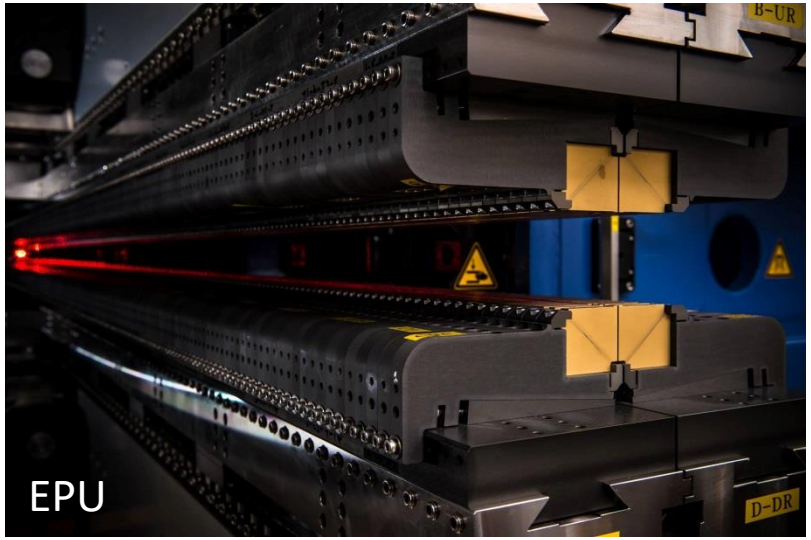

Analytic Methods

The magnetic field B_y+iB_x is expressed in polynomial expansions as

$$B_y + iB_x = \sum (b_n + ia_n)(x+iy)^n \quad (1)$$

The equation is divided into real part B_y and imaginary part B_x

$$B_y(x,y) = b_0 + a_1 y + b_1 x + 2a_2 xy + b_2(x^2 - y^2) + \ldots \quad (2)$$

$$B_x(x,y) = a_0 + a_1 x - b_1 y - 2b_2 xy + a_2(x^2 - y^2) + \ldots \quad (3)$$

b_0:normal dipole term
b_1:normal quadrupole term

a_0:skew dipole term
a_1:skew quadrupole term

Polynomial fit

Data Format

X_1, Y_1, By_1
X_2, Y_2, By_2
X_3, Y_3, By_3
.
.
.
X_j, Y_j, By_j

Choose fitting number *n*

$$B_y(x,y) = b_0 + a_1 y + b_1 x + 2a_2 xy + b_2(x^2 - y^2) + \ldots$$

b_0, a_0
b_1, a_1
b_2, a_2
b_3, a_3
.
.
.
b_n, a_n

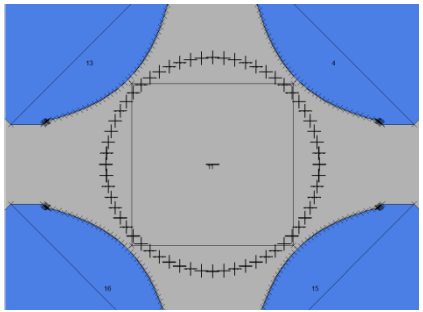

A circle path divided to j points

X_1, Y_1, Bx_1
X_2, Y_2, Bx_2
X_3, Y_3, Bx_3
.
.
.
X_j, Y_j, Bx_j

$$B_x(x,y) = a_0 + a_1 x - b_1 y - 2b_2 xy + a_2(x^2 - y^2) + \ldots$$

b_0, a_0
b_1, a_1
b_2, a_2
b_3, a_3
.
.
.
b_n, a_n

FFT

Data Format

θ_1, By_1
θ_2, By_2
θ_3, By_3
.
.
.
θ_j, By_j

$$By+iBx=\Sigma(b_n+ia_n)r^n e^{in\theta}$$
$$By(\theta)=\Sigma r^n[b_n\cos(n\theta)-a_n\sin(n\theta)]$$

Fast Fourier transfer

j points can define *n* number

b_0, a_0
b_1, a_1
b_2, a_2
b_3, a_3
.
.
.
b_n, a_n

A circle path divided to *j* points

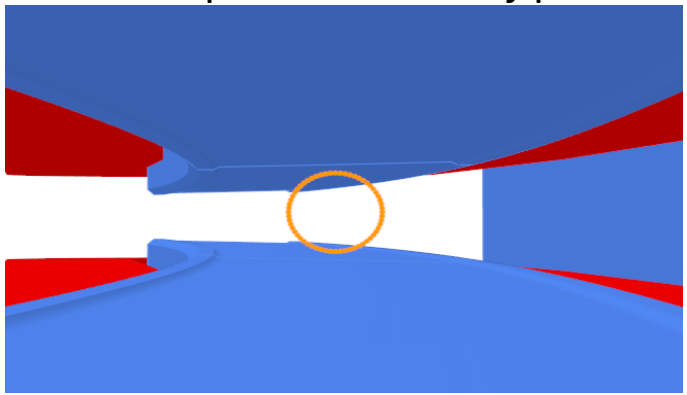

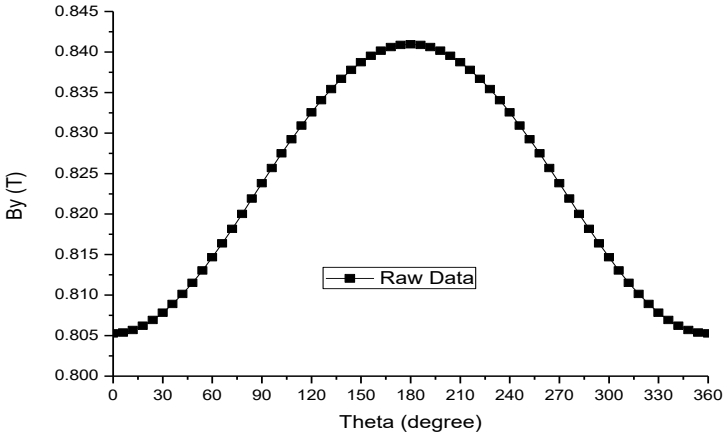

Pierre Schnizer

P.Schnizer et al. "*Theory and Application of Plane Elliptic multipoles for Static Magnetic Fields*", NIMA 607(3):505-516, 2009

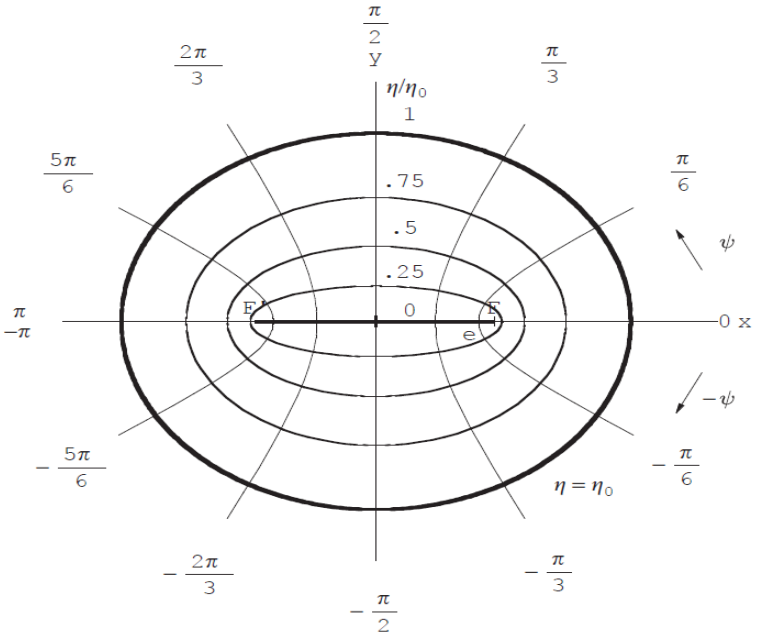

Fig. 1. Plane elliptic coordinates η, ψ, Foci F, F' are at $x = \pm e$.

$$x = e\cosh\eta\cos\psi, \quad 0 \le \eta < \infty$$
$$y = e\sinh\eta\sin\psi, \quad -\pi \le \psi \le \pi. \tag{13}$$

$$\mathbf{B}(\mathbf{z}) := B_y + iB_x$$

$$\mathbf{B}(\mathbf{z})/\mathscr{B}_0 = \sum_{m=0}^{\infty} \mathbf{C}_m \left(\frac{r}{R}\right)^m e^{im\theta} = \sum_{m=0}^{\infty} \mathbf{C}_m \left(\frac{x+iy}{R}\right)^m. \tag{8}$$

$$\mathbf{C}_m = \frac{1}{2\pi}\int_{-\pi}^{\pi} \frac{\mathbf{B}_0(\theta)}{\mathscr{B}_0} e^{-im\theta}\, d\theta. \tag{9}$$

Circular multipoles

$$\mathbf{B}/\mathscr{B}_0 = \frac{\mathbf{E_0}}{2} + \sum_{n=1}^{\infty} \mathbf{E}_n \frac{\cosh[n(\eta + i\psi)]}{\cosh(n\eta_0)}. \tag{24}$$

$$\mathbf{E}_n = \frac{1}{\pi\mathscr{B}_0}\int_{-\pi}^{\pi} \mathbf{B}_0(\mathbf{z} = e\cosh(\eta_0 + i\psi))\cos(n\psi)\, d\psi \tag{27}$$

Elliptical multipoles

$$\mathbf{B}(\mathbf{z})/\mathscr{B}_0 = \sum_{m=0}^{\infty} \mathbf{C}_m \left(\frac{x+iy}{R}\right)^m = \sum_{m=0}^{\infty} \mathbf{C}_m \alpha^m \cosh^m \mathbf{w} \tag{29}$$

$$\alpha^m \mathbf{C}_m = \sum_{k=0}^{\infty} \mathbf{E}_k/[(1+\delta_{k0})\cosh(k\eta_0)]t_{km},$$
$$k, m = 0, 1, 2, \ldots. \tag{34}$$

$$m = \text{even}: \; t_{km} = (-1)^{m/2}\cos(k\pi/2)\frac{1}{m!} \times \Pi_{\mu=1}^{m/2}(k^2 - [2(\mu-1)]^2) \tag{36}$$

$$m = \text{odd}: \; t_{km} = (-1)^{(m-1)/2}\sin(k\pi/2)\frac{k}{m!} \times \Pi_{\mu=1}^{(m-1)/2}(k^2 - (2\mu-1)^2). \tag{37}$$

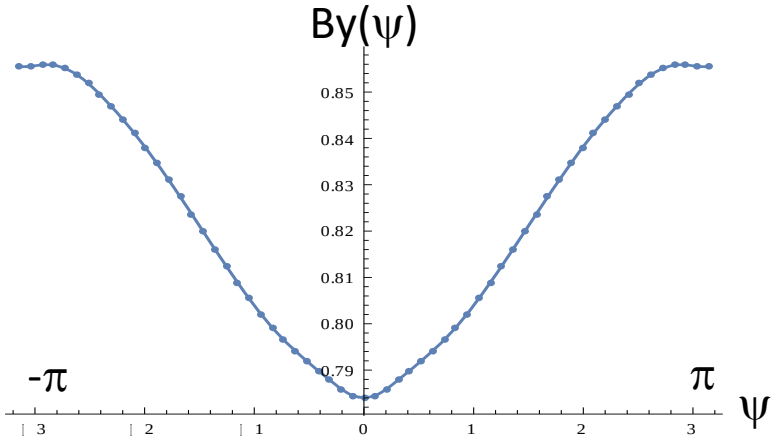

Ra=20mm **semi-major axis**

Rb=8mm **semi-minor axis**

r=15mm **radius of circular multipoles expansion**

$$m = \text{even}: \quad t_{km} = (-1)^{m/2} \cos(k\pi/2) \frac{1}{m!} \times \Pi_{\mu=1}^{m/2} (k^2 - [2(\mu-1)]^2) \tag{36}$$

$$m = \text{odd}: \quad t_{km} = (-1)^{(m-1)/2} \sin(k\pi/2) \frac{k}{m!} \times \Pi_{\mu=1}^{(m-1)/2} (k^2 - (2\mu-1)^2). \tag{37}$$

Transfer matrix of even multipoles from elliptical multipoles to circular multipoles

Out[25]//MatrixForm=

m=even: t_{km}=

1/2	-0.724138	0.355359	-0.156465	0.0673952	-0.0289105	0.0123923	-0.00531116	0.00227622	-0.000975526
0	0.969828	-1.90371	1.88596	-1.44418	0.967985	-0.597487	0.348545	-0.195105	0.105827
0	0	1.2748	-3.36779	4.83543	-5.18563	4.66787	-3.73441	2.74366	-1.88977
0	0	0	1.50348	-5.18082	9.72306	-13.3368	15.0043	-14.6982	12.9922
0	0	0	0	1.73465	-7.44112	17.2238	-28.7073	38.6671	-44.7434
0	0	0	0	0	1.99316	-10.2523	28.1946	-55.2388	86.5573
0	0	0	0	0	0	2.28845	-13.7311	43.7157	-98.3605
0	0	0	0	0	0	0	2.62713	-18.0147	65.1426
0	0	0	0	0	0	0	0	3.01586	-23.2652
0	0	0	0	0	0	0	0	0	3.46209

Transfer matrix of odd multipoles from elliptical multipoles to circular multipoles

Out[31]//MatrixForm=

m=odd: t_{km}=

0.75	-1.27703	0.969941	-0.588815	0.325152	-0.170386	0.0863055	-0.0426791	0.0207299	-0.00992946
0	1.1402	-2.59806	3.15437	-2.90315	2.28195	-1.61823	1.06698	-0.666319	0.398952
0	0	1.39182	-4.2246	6.99865	-8.55732	8.66908	-7.71654	6.24674	-4.70193
0	0	0	1.61656	-6.2488	13.0979	-19.9035	24.6063	-26.2937	25.1889
0	0	0	0	1.85976	-8.77094	22.2137	-40.2782	58.6912	-73.0928
0	0	0	0	0	2.13578	-11.9002	35.3088	-74.3168	124.59
0	0	0	0	0	0	2.45197	-15.7629	53.5939	-128.355
0	0	0	0	0	0	0	2.8148	-20.5079	78.5848
0	0	0	0	0	0	0	0	3.23128	-26.3119
0	0	0	0	0	0	0	0	0	3.70938

Out[40]//MatrixForm=

Number of circular multipole	Value
0	0.823442
1	-1.78526
2	-3.34124
3	10.8776
4	815.01
5	-24 229.7
6	-8.42796×10^{6}
7	2.9995×10^{8}
8	1.35615×10^{10}
9	-3.02063×10^{12}
10	-4.08203×10^{14}
11	1.38306×10^{16}
12	3.82107×10^{18}
13	1.84429×10^{19}
14	-4.85593×10^{22}
15	-1.19821×10^{24}
16	4.60038×10^{26}
17	1.357×10^{28}
18	-3.19484×10^{30}
19	-9.45785×10^{31}
20	1.6015×10^{34}
21	4.57078×10^{35}
22	-5.70995×10^{37}
23	-1.55765×10^{39}
24	1.40731×10^{41}
25	3.67578×10^{42}
26	-2.26729×10^{44}
27	-5.72312×10^{45}
28	2.132×10^{47}
29	5.29547×10^{48}
30	-8.78788×10^{49}
31	-2.20595×10^{51}

$$\alpha^m \mathbf{C}_m = \sum_{k=0}^{\infty} \mathbf{E}_k / [(1+\delta_{k0})\cosh(k\eta_0)] t_{km},$$
$$k, m = 0, 1, 2, \ldots . \qquad (34)$$

Simulation Case
Circular path data of a combined dipole

Simulation of Multipoles in a circle

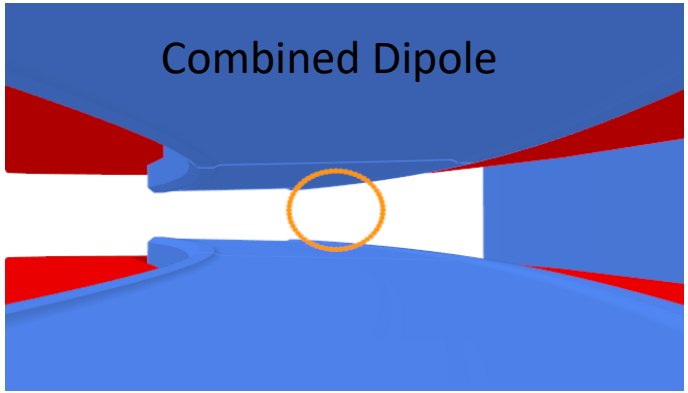

Combined Dipole	Main components	Normalize to $b_0(x10^{-4})$ @10mm
b_0	0.823 T	10000
b_1	-1.79 T/m	-216.8
b_2	-3.38 T/m^2	-4.1

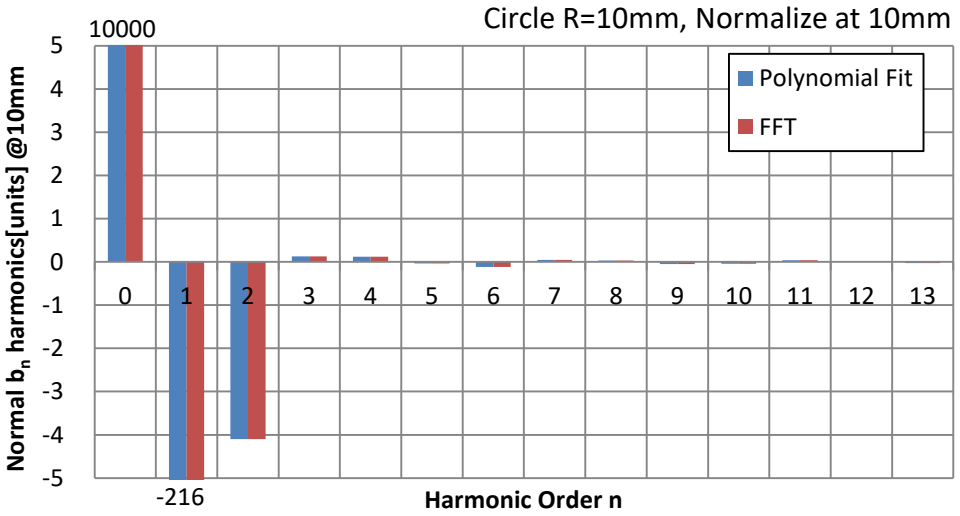

- The multipole results of polynomial fit and FFT are the same in a circular path at a combined dipole.
- Shows two analysis methods are consistence in a circular path.

Circle	Polynomial	FFT
b_0	0.8234427 T	0.823443 T
b_1	-1.785341 T/m	-1.785342 T/m
b_2	-3.376005 T/m^2	-3.375895 T/m^2

Combined Dipole Magnet

Circular Path

R=10mm

b_n 、a_n into

$By(\theta)=\Sigma r^n[b_n\cos(n\theta)-a_n\sin(n\theta)]$

or

$By(x,y)=b_0+a_1y+b_1x+2a_2xy+b_2(x^2-y^2)+...$

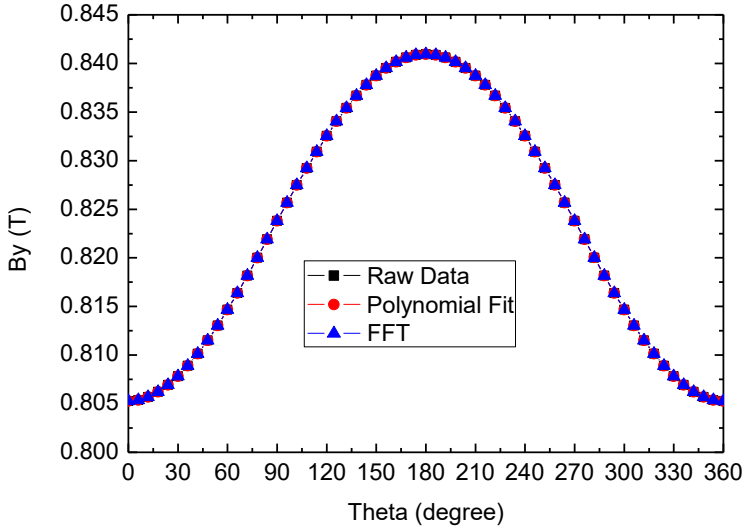

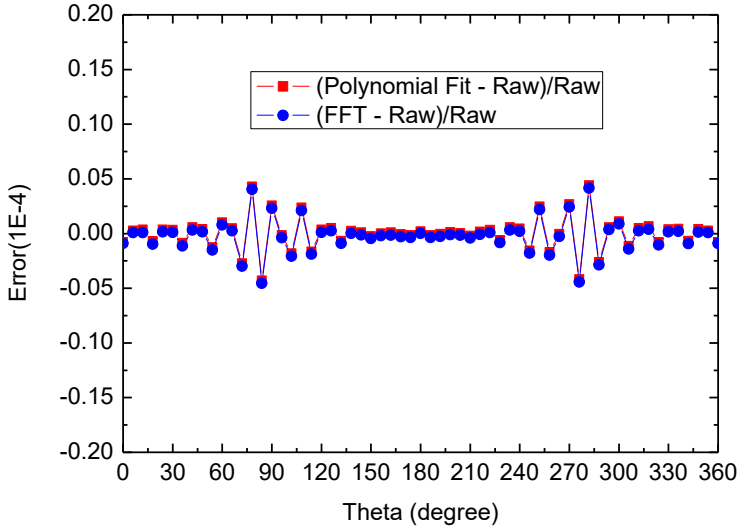

- The errors of these two methods are within $5x10^{-6}$.

Simulation Case
Elliptical path data of a combined dipole

Elliptical Path Analysis

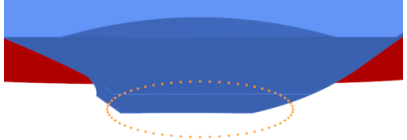

Combined Dipole

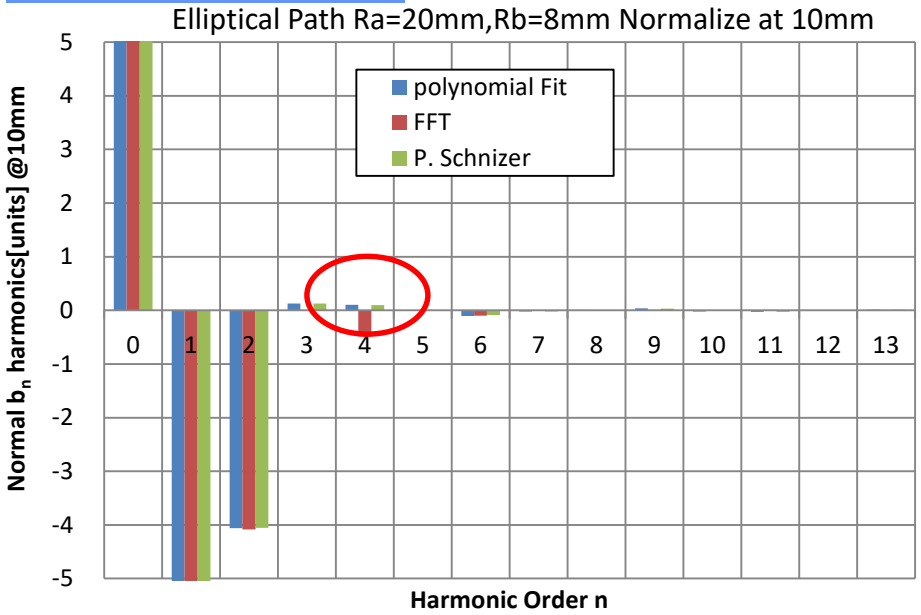

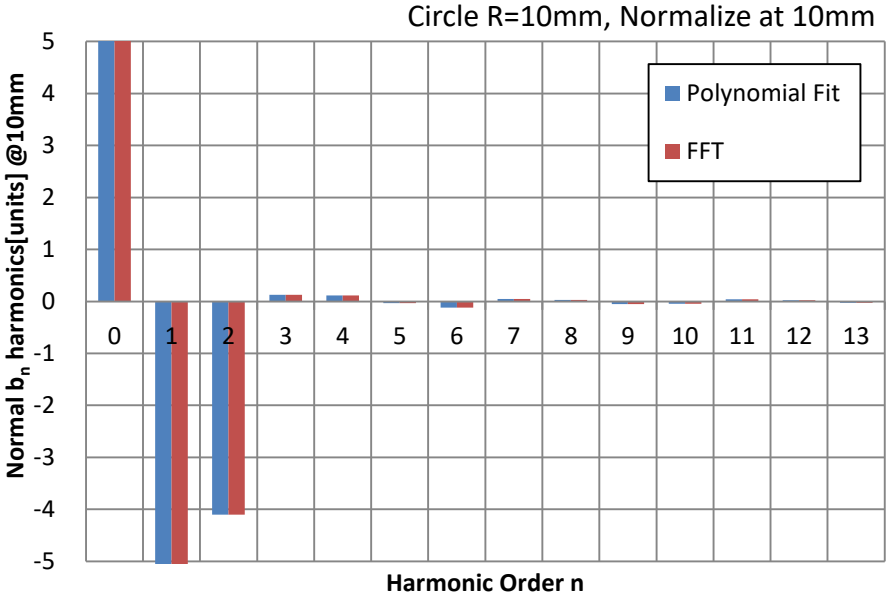

Ellipse	Polynomial	FFT	P. Schnizer
b_0	0.8234423 T	0.822633 T	0.823442 T
b_1	-1.785267 T/m	-1.784512 T/m	-1.78526 T/m
b_2	-3.341436 T/m^2	-3.359222 T/m^2	-3.34125 T/m^2

Circle	Polynomial	FFT
b_0	0.8234427 T	0.823443 T
b_1	-1.785341 T/m	-1.785342 T/m
b_2	-3.376005 T/m^2	-3.375895 T/m^2

Elliptical path b_n 、 a_n into

$By(x,y)=b_0+a_1y+b_1x+2a_2xy+b_2(x^2-y^2)+...$

Combined Dipole

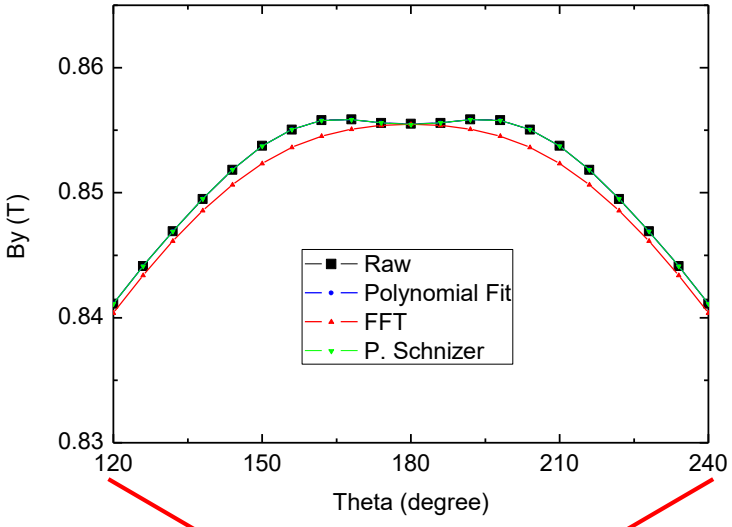

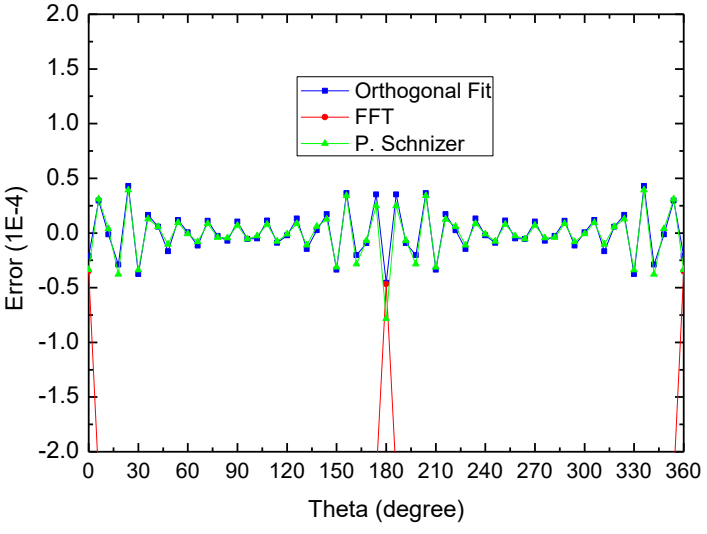

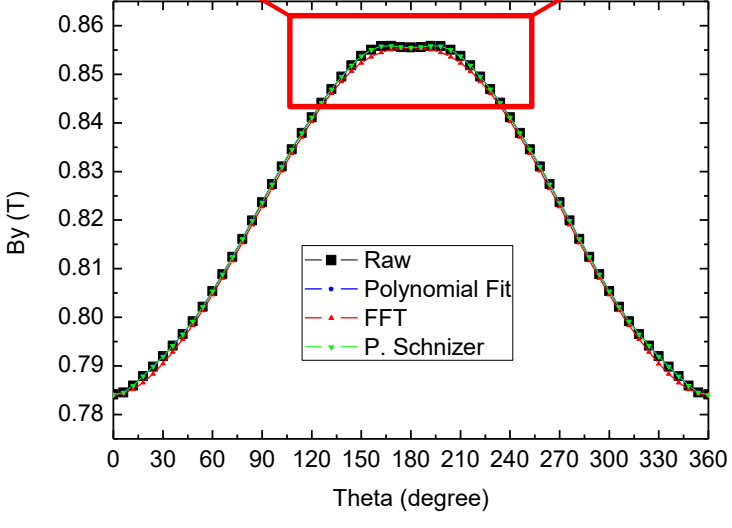

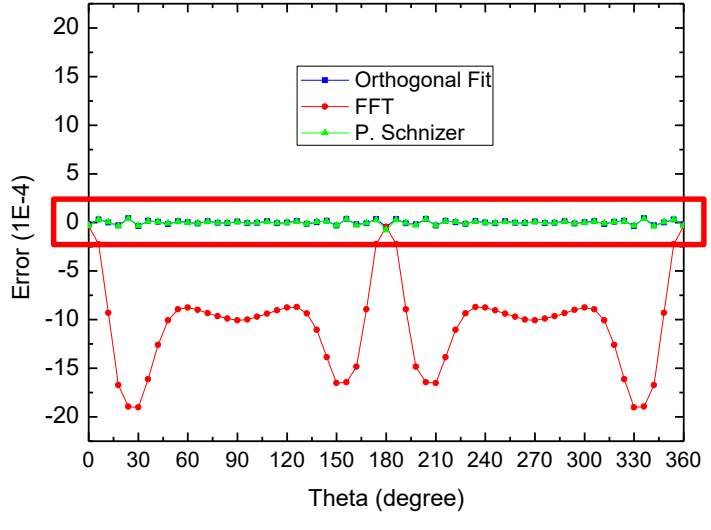

Analysis Conclusion

- The multipole results of polynomial fit and FFT are the same in a circular path at a combined dipole. The errors of these two methods are within $5x10^{-6}$.
- Polynomial fit, FFT and P. Schnizer in an ellipse are compared, polynomial fit result is the same as P. Schnizer, FFT multipole got a large errors. So we can chose polynomial fit or P. Schnizer anaylsis method for multipoles in an ellipse.
- The fitting errors of polynomial fit and P. Schnizer of elliptical path are within $5x10^{-5}$.

Stretched wire system

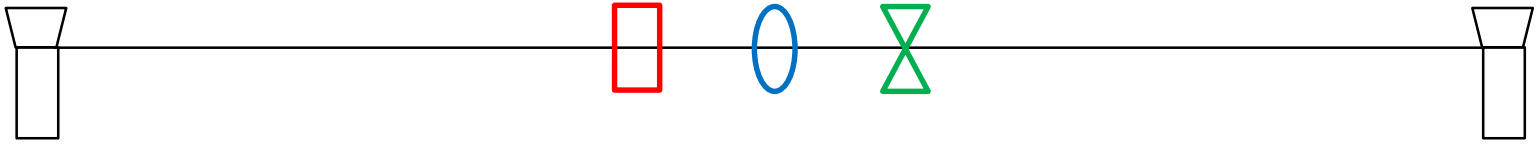

Stretched Wire System Setup

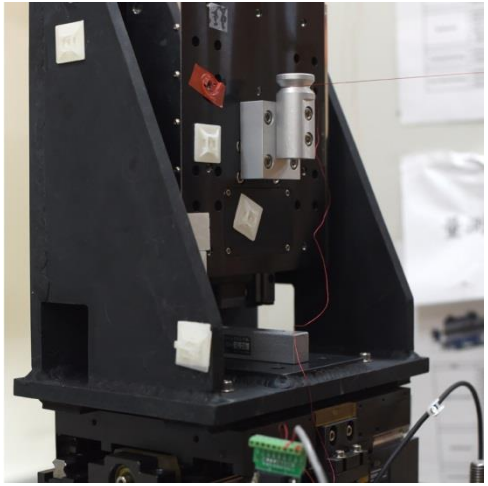

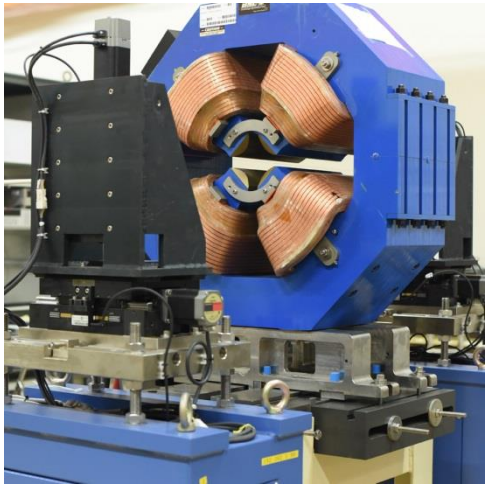

Parameter	Value	Units
Wire length	1100	mm
Wire diameter	0.3	mm
Wire mass density	0.4	g/m
Wire sag	0.25	mm

Parameters of 8 turns copper wires.

- Integrator and voltmeter (Keithley2182) testing results are very close.
- The movement of transverse and vertical direction are moving by stepping motors.
- The wires are stretched by moving the stage longitudinal manually.
- Mechanical centre can be found by level meter and theodolite.
- 8 turns copper wires are in series.

Standard deviation at one position

STDEV	Voltmeter KEITHLEY 2182	Integrator FDI 2056
Be-Cu wire dx=2mm	3.0 G-cm	2.9 G-cm
Be-Cu wire dx=4mm	2.0 G-cm	-
8 Cu wires dx=2mm	1.0 G-cm	1.0 G-cm
8 Cu wires dx=4mm	0.5 G-cm	0.5 G-cm

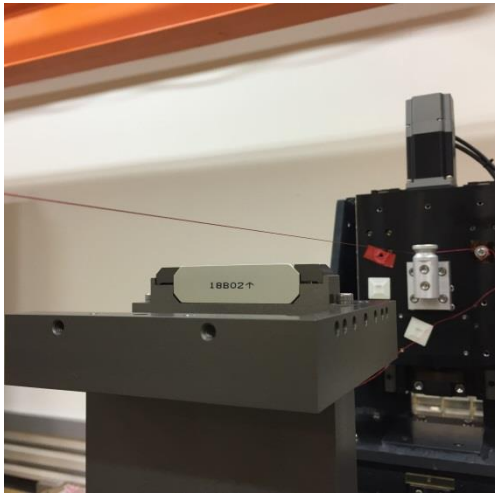

Ref. NdFeB Block
By(x=0mm)=3300 G-cm

Move step dx (mm)	STDEV (G-cm)
1	2
2	1
4	0.5
6	0.2
8	0.3

8Cu wires
With FDI2056
v=25 mm/s

Poor space resolution

Integral multipoles of a quadrupole magnet by stretched wire system

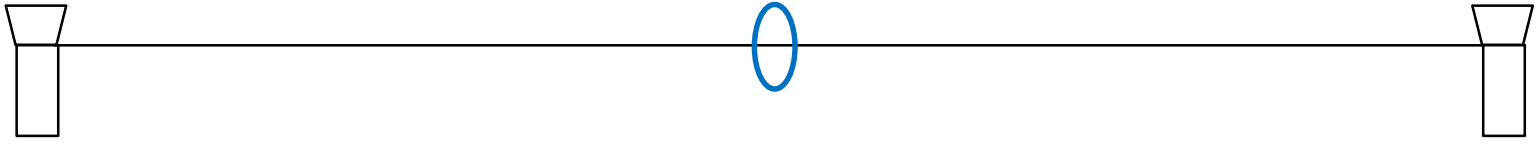

QM R25mm HPS & SW Experimental Results

Normal bn harmonics

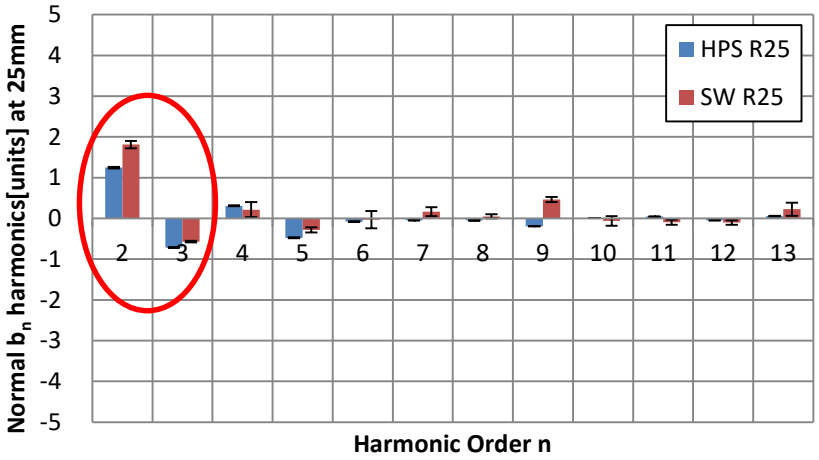

Skew an harmonics

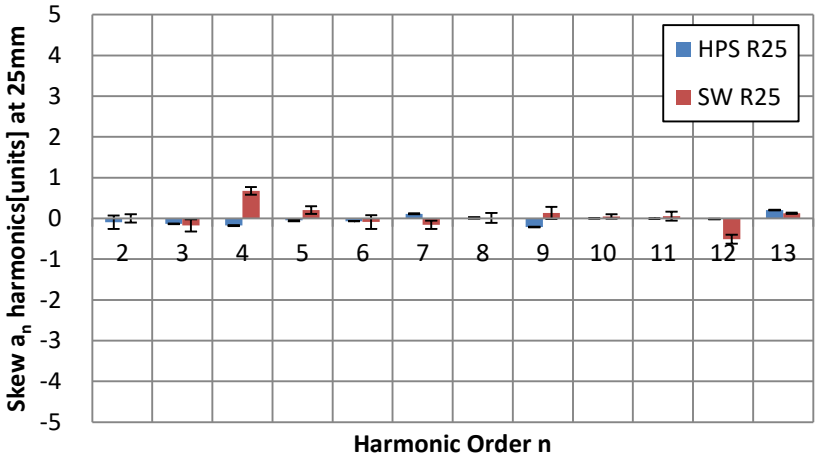

Circle R=25mm, Normalize at 25mm

System	∫Gdz (T)
HPS	5.178
SW	5.179

- Normal sextupole(b2) and octupole (b3) are particular multipole.
- The difference of all multipole are within 1 units between HPS and SW.

R25mm HPS vs SW

QM

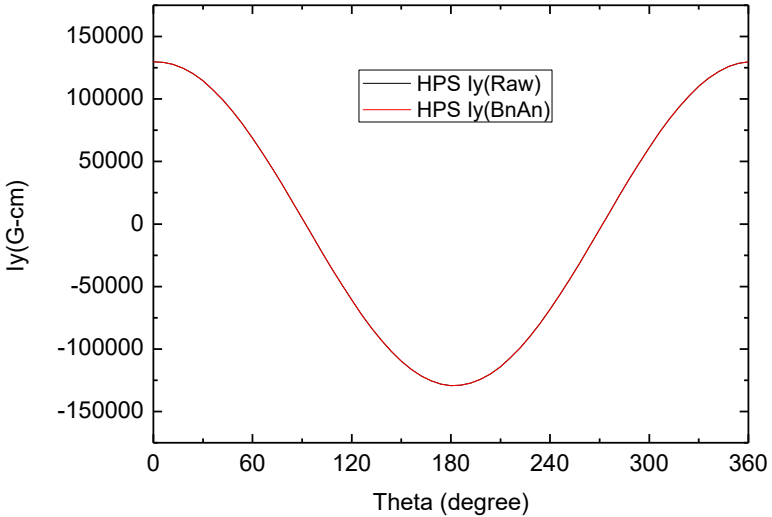

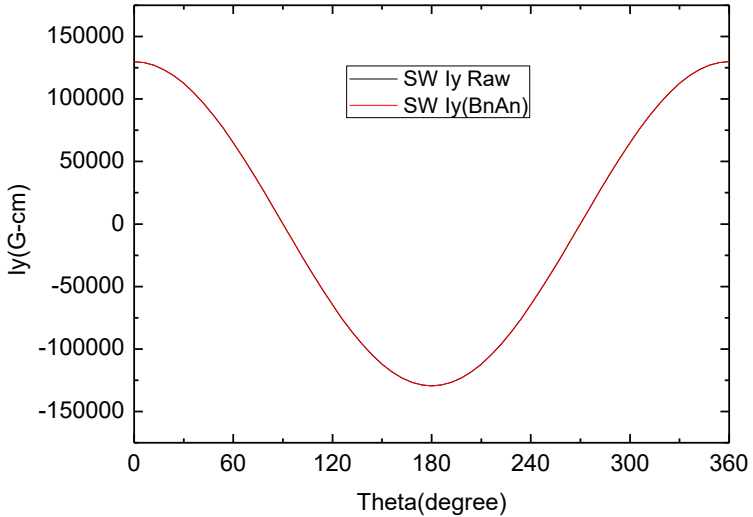

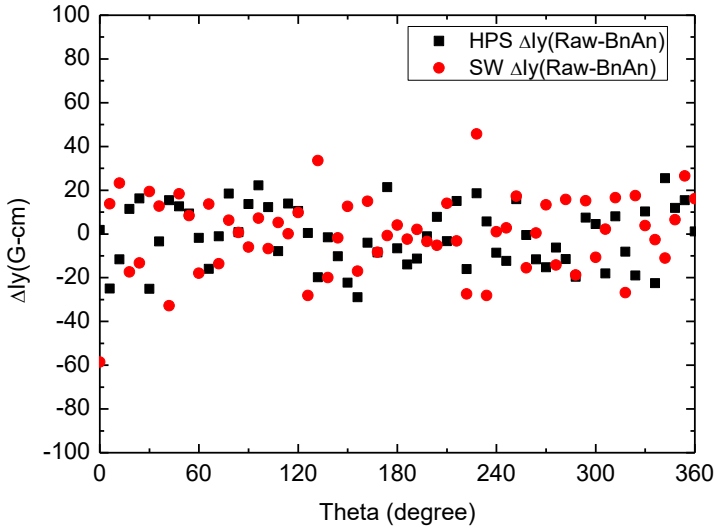

R5mm HPS vs SW

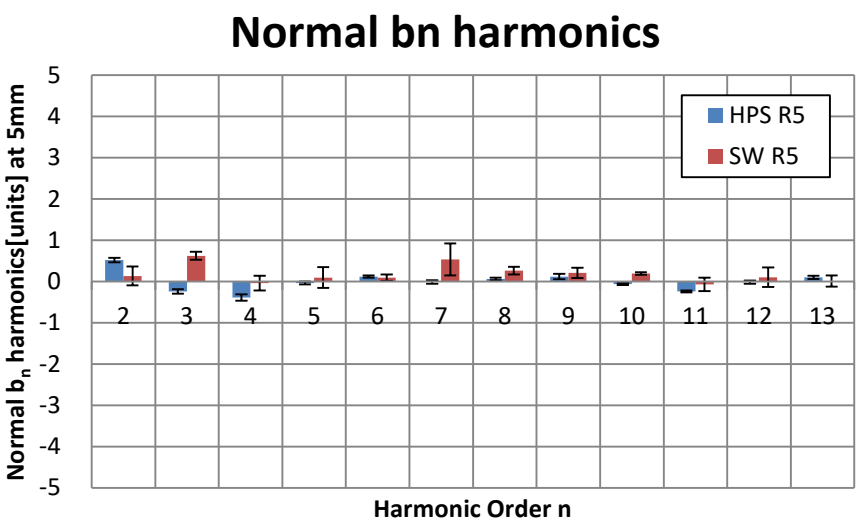

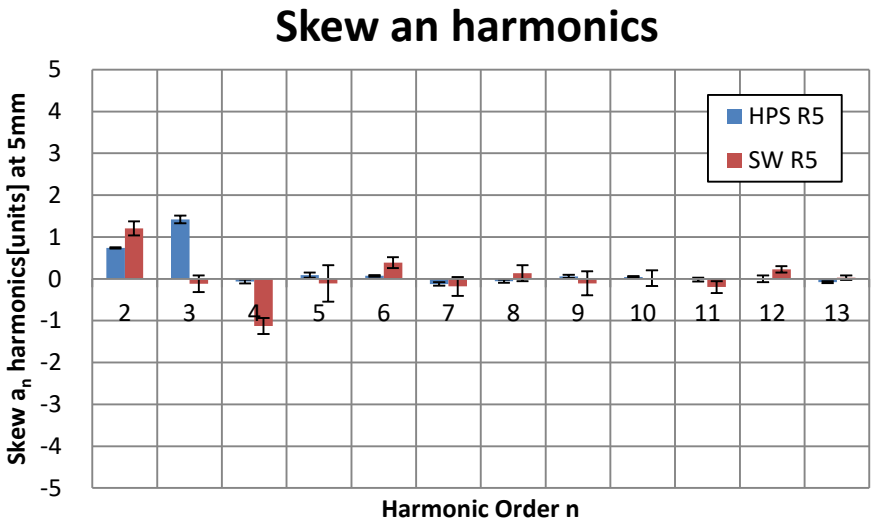

Circle R=5mm, Normalize at 5mm

System	∫Gdz (T)
HPS	5.177
SW	5.178

- The deviation of R5 data is larger than R25.
- The difference is within 2 units between HPS and SW.

Elliptical Path HPS vs SW

QM

Normal bn harmonics

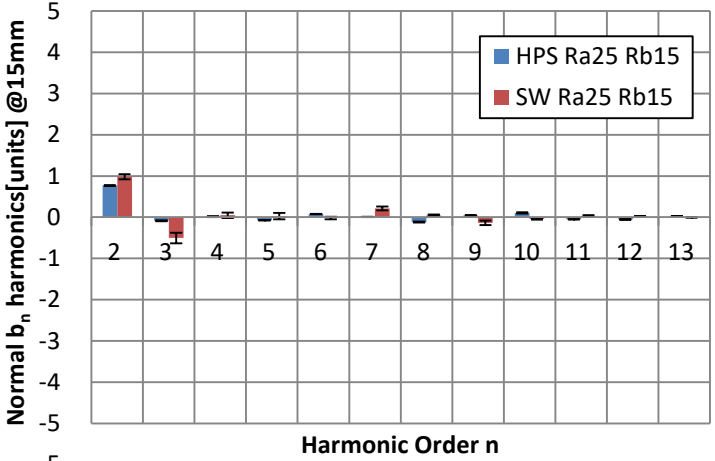

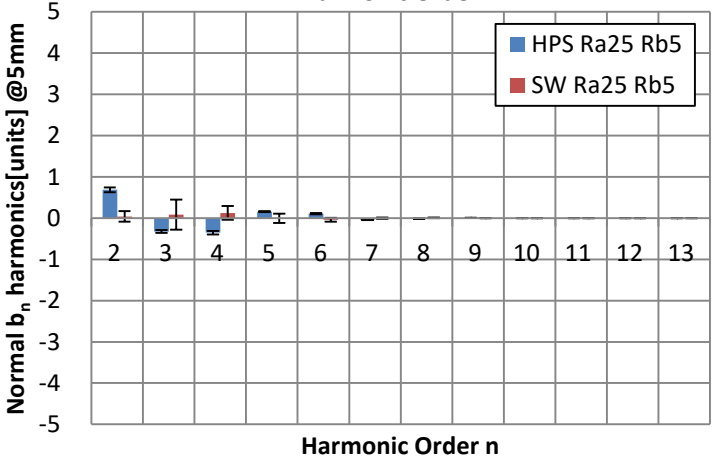

Skew an harmonics

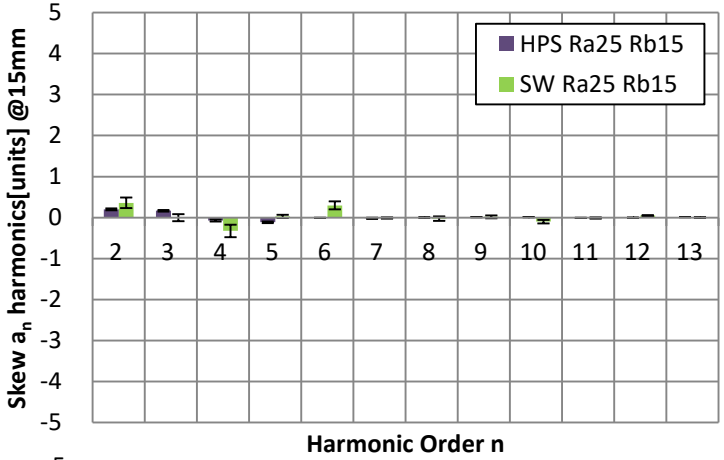

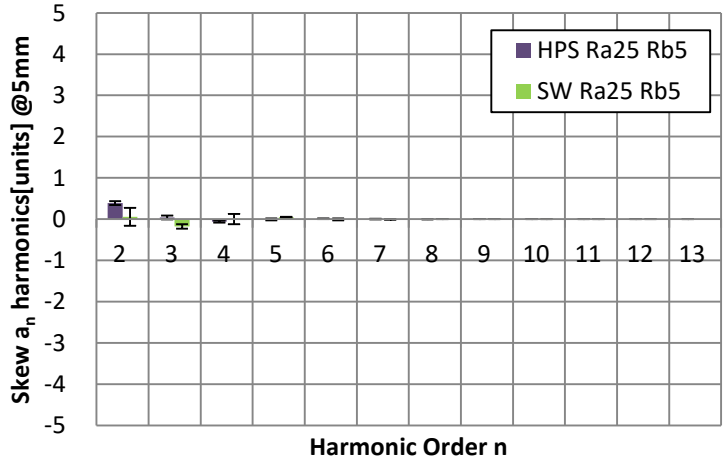

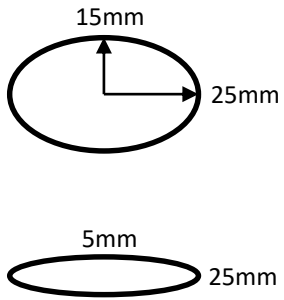

HPS/SW Path	∫Gdz (T)
HPS Ellipse Ra25 Rb15	5.177
HPS Ellipse Ra25 Rb5	5.176
SW Ellipse Ra25 Rb15	5.174
SW Ellipse Ra25 Rb5	5.176

Normalize at short axis radius

Integral multipoles of in-vacuum undulator by stretched wire system

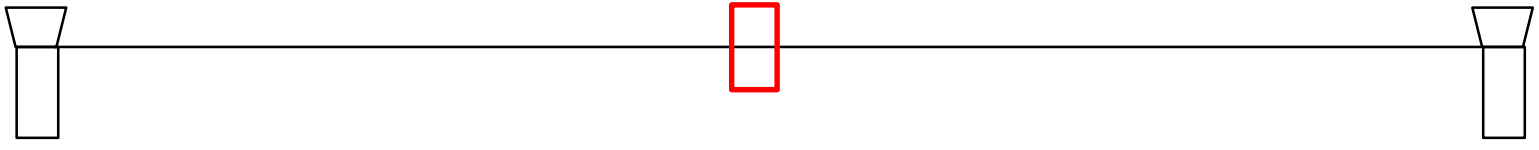

IU24 Linear & Elliptical measurement

To check skew quadrupole value which is out of spec.

-15 < x < 15 (mm)		Linear Measurement		
Gap(mm)		Dipole(n=0)	Quadrupole(n=1)	Sextupole(n=2)
Spec.		**≤100 G-cm**	**≤50 G**	**≤100 G/cm**
6.8	Normal(Iy)	-3.9	34.1	14.1
	Skew(Ix)	62.2	-79.8	-8.1
7	Normal(Iy)	-11.7	38.5	15.4
	Skew(Ix)	50.5	-82.3	16.7
8	Normal(Iy)	-28.9	26.3	14.6
	Skew(Ix)	48.8	-60.2	18.5
9	Normal(Iy)	-38.8	29.6	16.2
	Skew(Ix)	52.4	-41.2	3.6

Elliptical Measurement				
Gap(mm)		Dipole(n=0)	Quadrupole(n=1)	Sextupole(n=2)
Spec.		**≤100 G-cm**	**≤50 G**	**≤100 G/cm**
6.8	Normal	0.4	47.1	43.1
	Skew	-	-105.7	29.8
7	Normal	-6.0	36.0	33.2
	Skew	-	-78.7	21.3
8	Normal	-21.8	48.5	68.0
	Skew	-	-73.4	16.1
9	Normal	-34.3	49.6	61.4
	Skew	-	-44.8	35.8

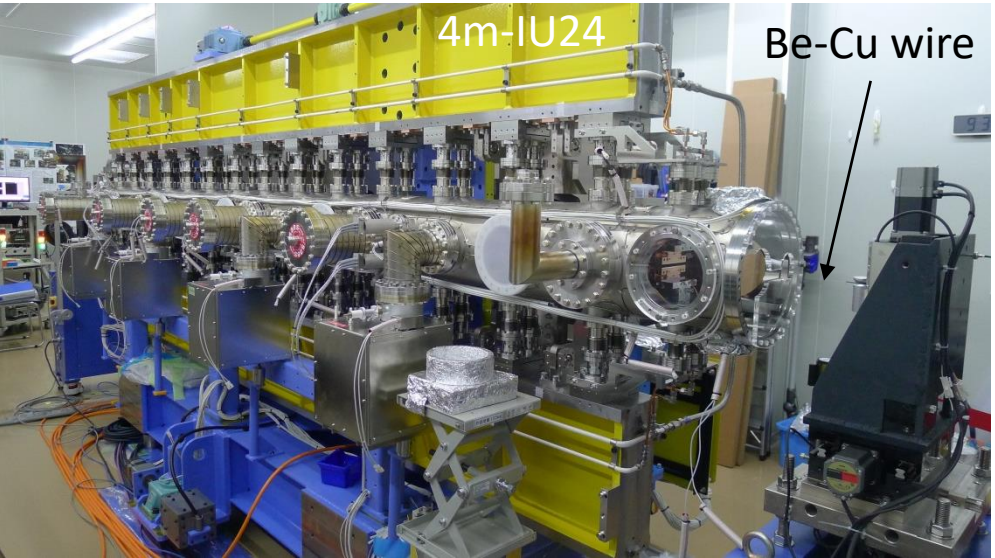

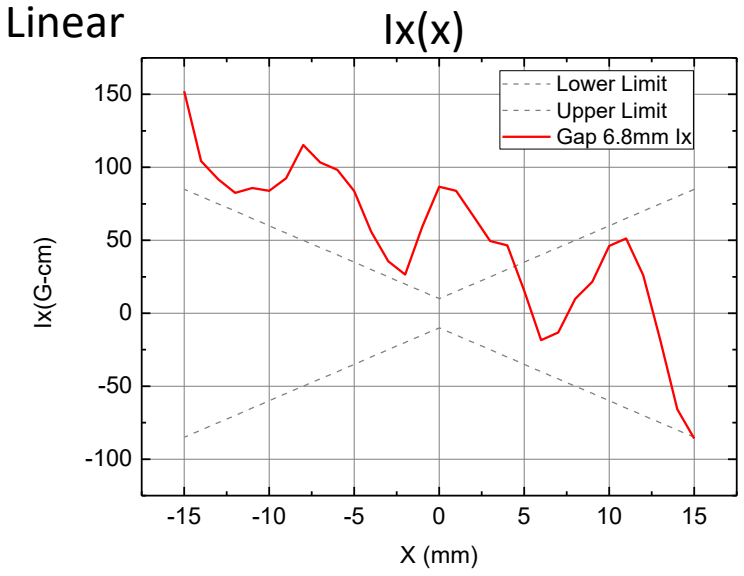

IU24 Gap 6.8mm

Linear

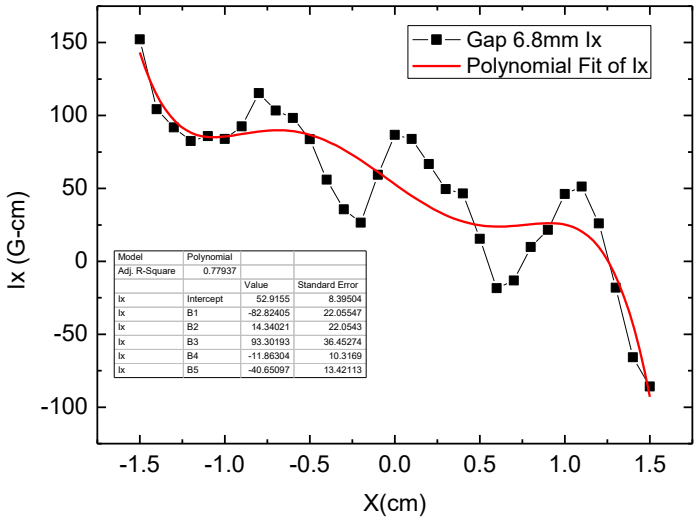

Model	Polynomial		
Adj. R-Square	0.77937		
		Value	Standard Error
Ix	Intercept	52.9155	8.39504
Ix	B1	-82.82405	22.05547
Ix	B2	14.34021	22.0543
Ix	B3	93.30193	36.45274
Ix	B4	-11.86304	10.3169
Ix	B5	-40.65097	13.42113

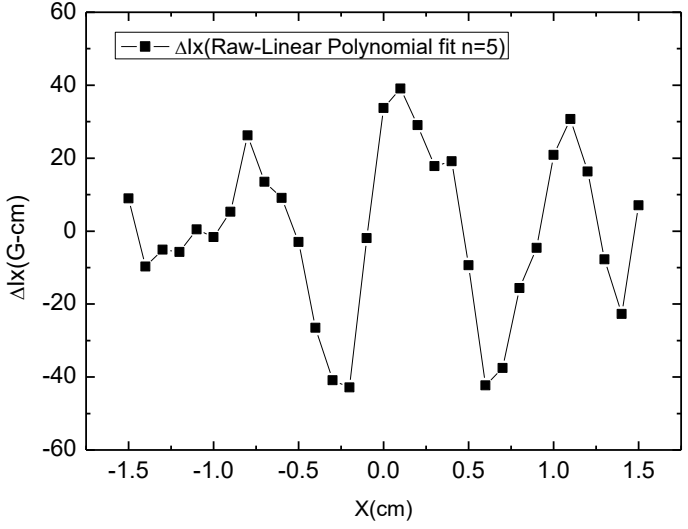

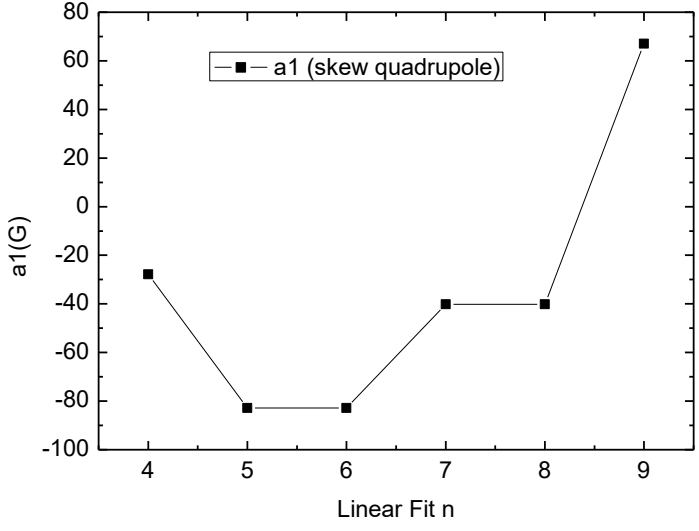

- It is hard to confirm skew quadrupole value.
- Different linear polynomial fit number get different results.

IU24 Gap 6.8mm

Elliptical path polynomial fit

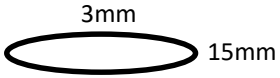

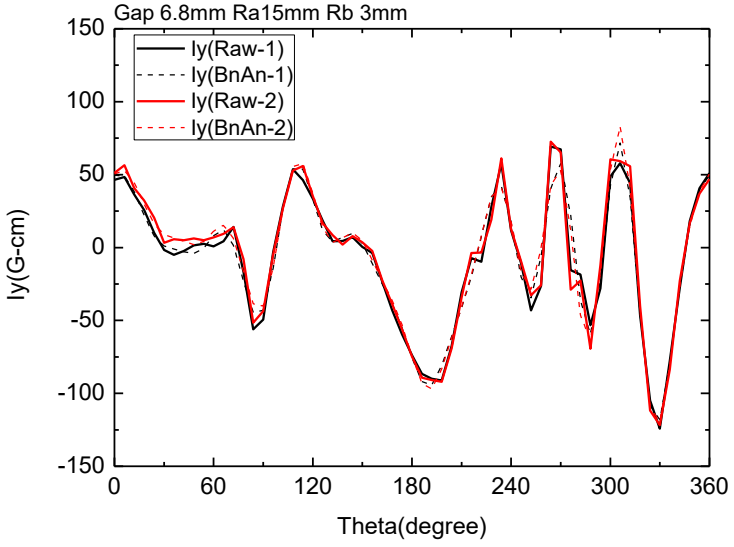

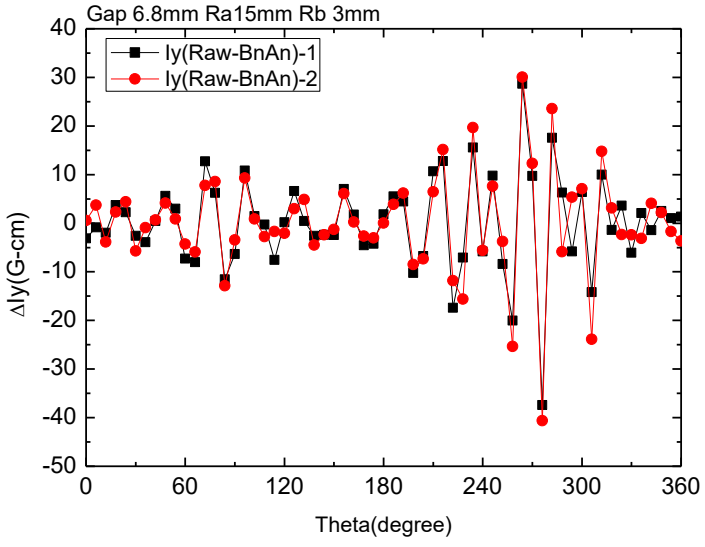

Raw data Iy(x,y) still was looked like unusually but elliptical path polynomial fit well.

IU24

N=6~14

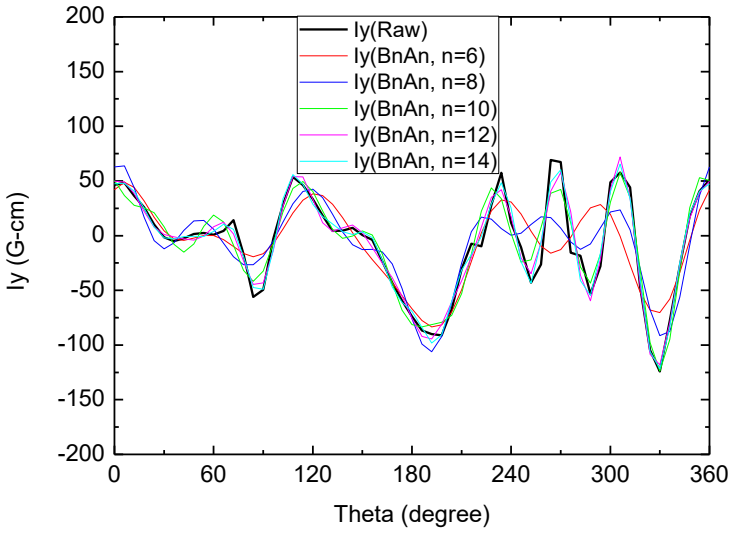

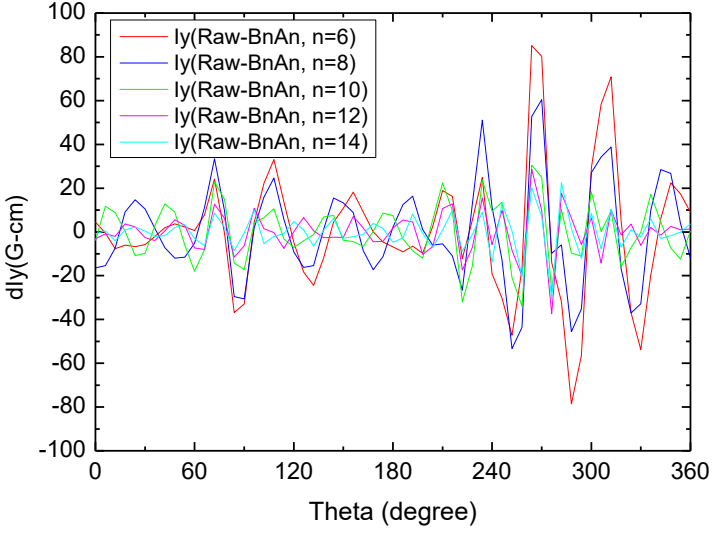

N=14~18

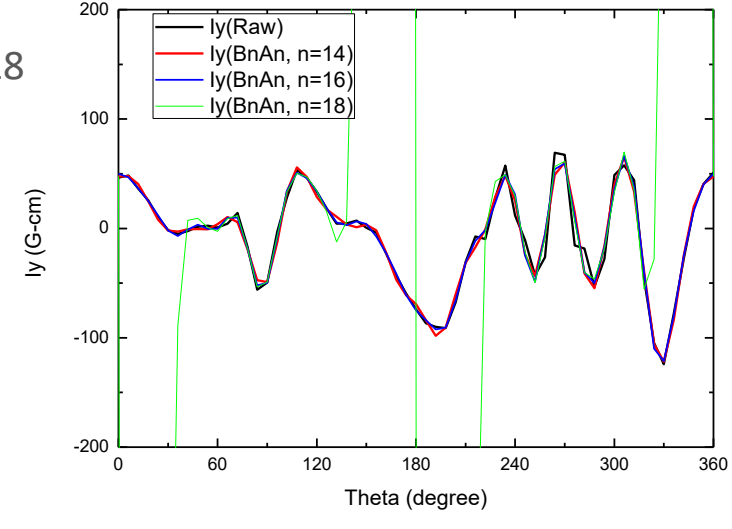

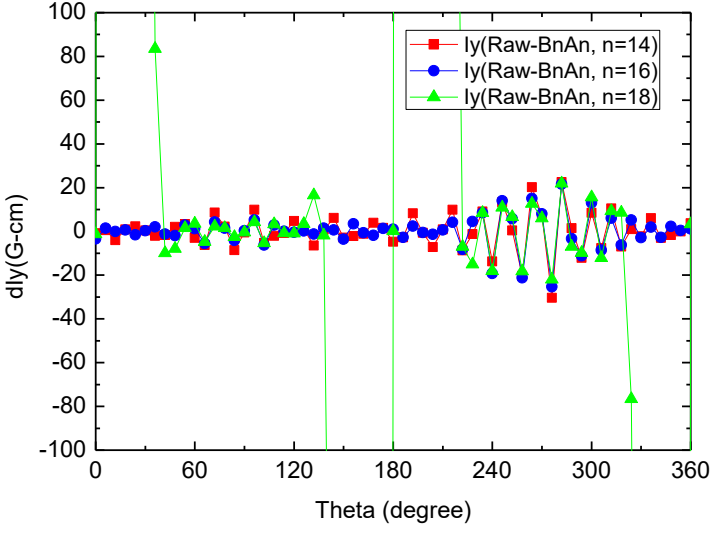

IU24

Normal Terms

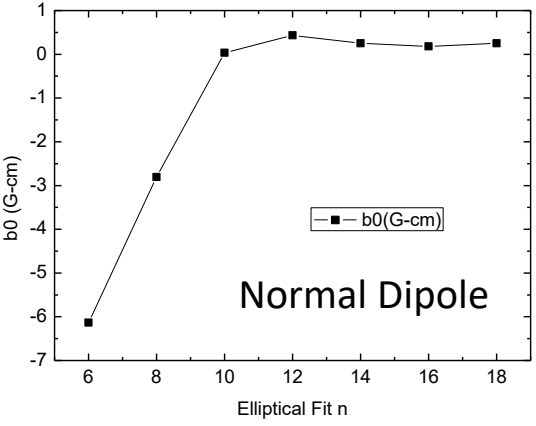

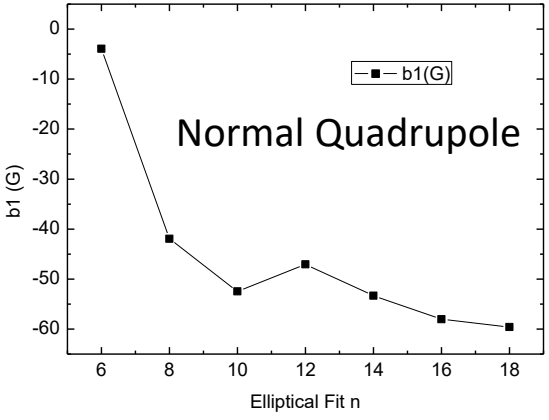

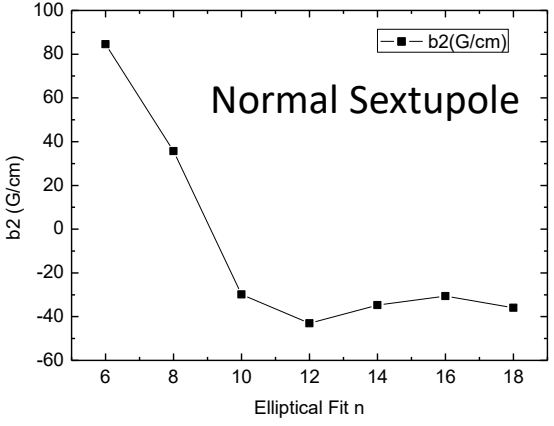

Skew Terms

b0, b1, b2, a1, a2 are convergent.

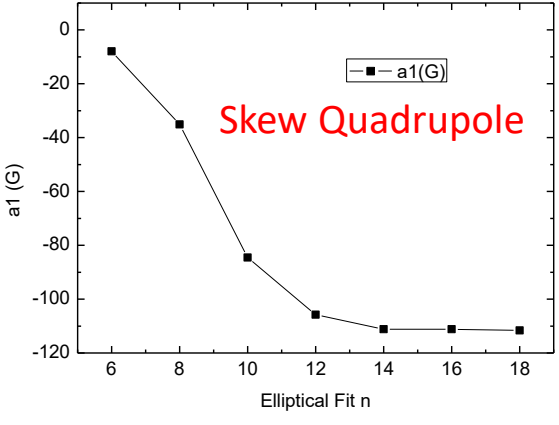

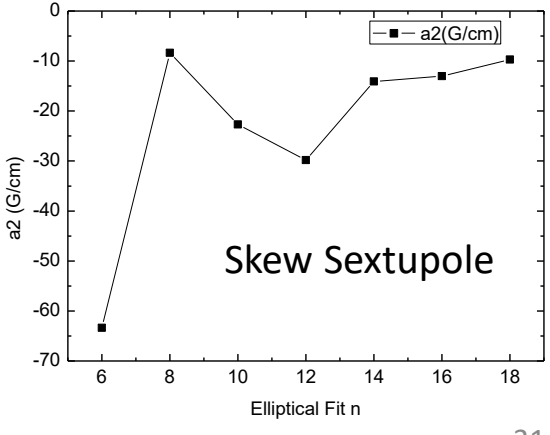

IU24 Gap 40mm Circle & Ellipse

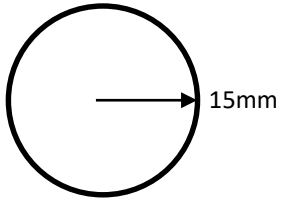

Circle				
Gap (mm)		Dipole (n=0)	Quadrupole (n=1)	Sextupole (n=2)
Spec.		**≤100 G-cm**	**≤50 G**	**≤100 G/cm**
40	Normal	3.59	7.40	4.95
	Skew	-	-52.42	-6.94

Ellipse				
Gap (mm)		Dipole (n=0)	Quadrupole (n=1)	Sextupole (n=2)
Spec.		**≤100 G-cm**	**≤50 G**	**≤100 G/cm**
40	Normal	3.74	5.69	1.59
	Skew	-	-53.85	-16.1

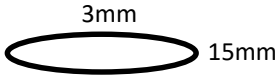

The multipole results are similar in a circle and ellipse.

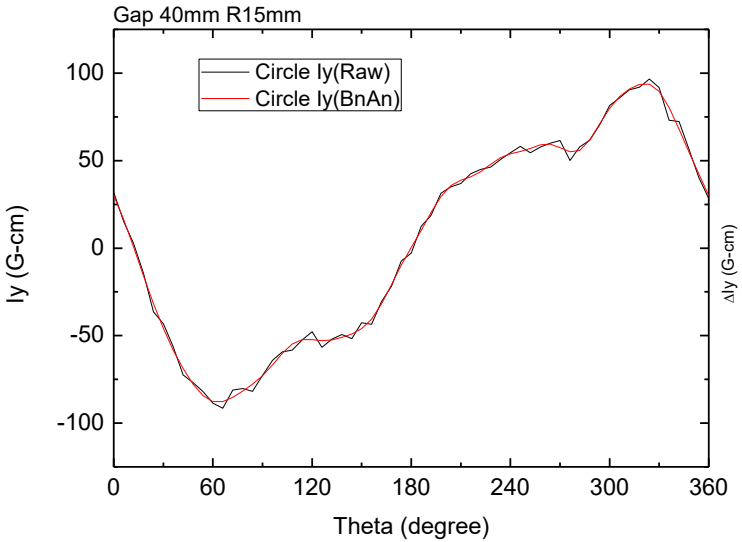

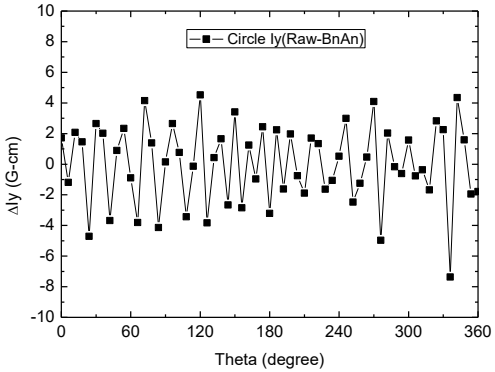

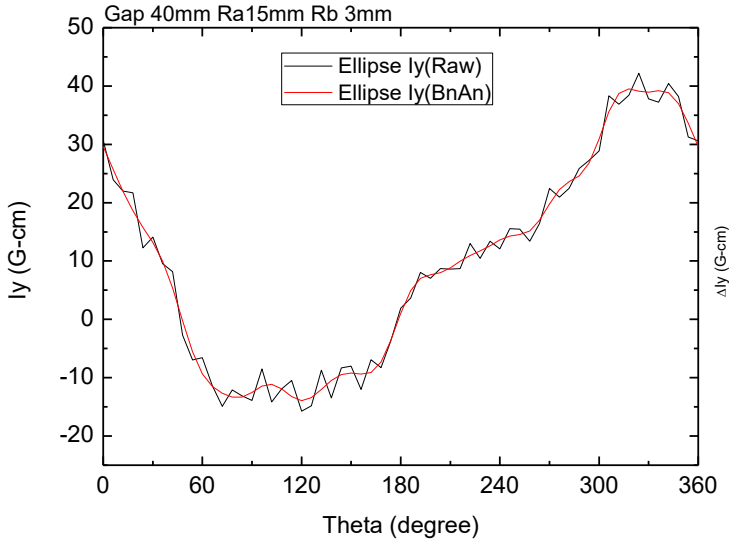

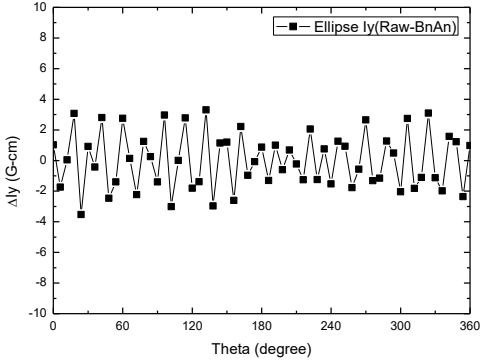

Conclusions

- A quadrupole magnet was measured by Hall probe system and stretched wire system and results were compared. Hall probe system can be more precise but stretched wire system can save lot of time.
- The difference of multipoles are within $2x10^{-4}$ between Hall probe system and stretched wire system.
- Circular and elliptical measurement of a quadrupole magnet multipoles are showed. If elliptical path multipoles normalized at short radius, the result is similar to circular path multipoles.
- Compare to linear measurement of in-vacuum undulator, elliptical path result shows more easy to confirm the main multipoles(n=0, 1, 2).
- Stretched wire system not only can measure 1^{st} and 2^{nd} integral fields but also can measure multipoles.

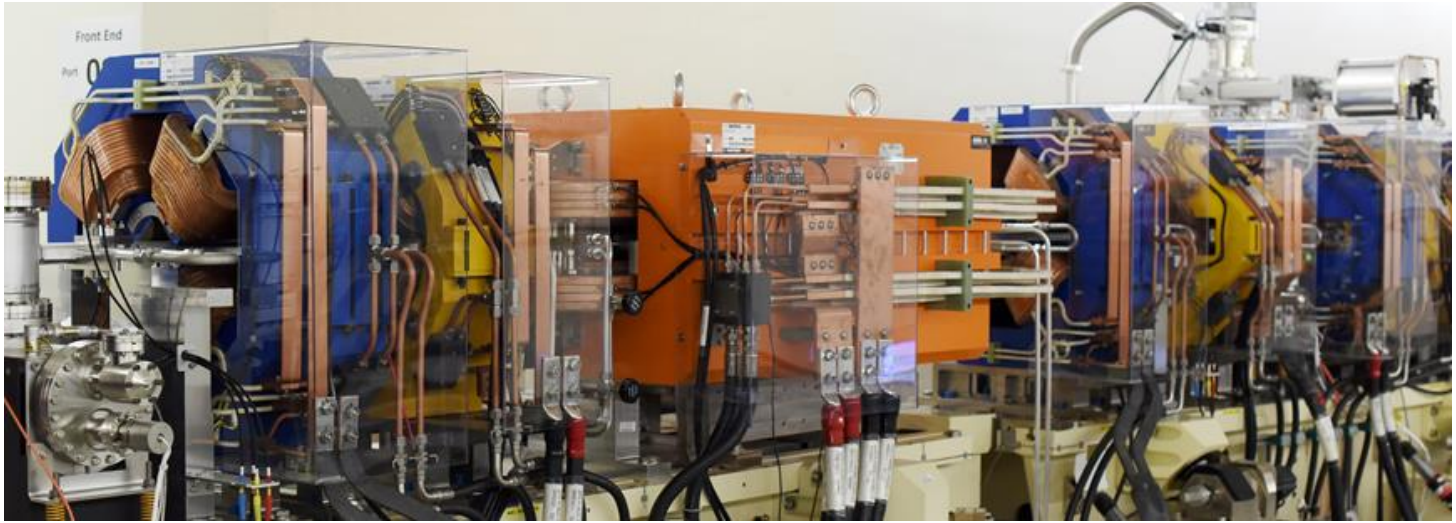

Many Thanks for Your Attention!

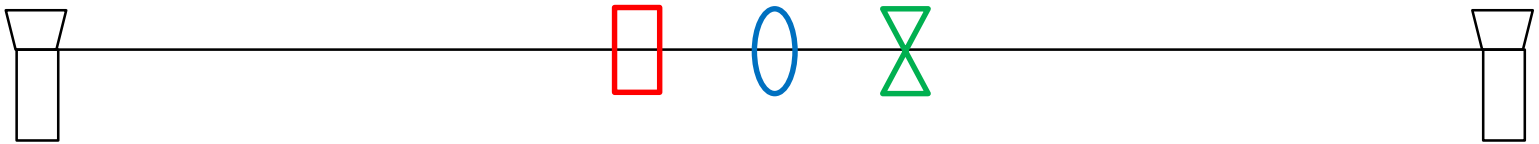

Circle R=10 Fitting Number

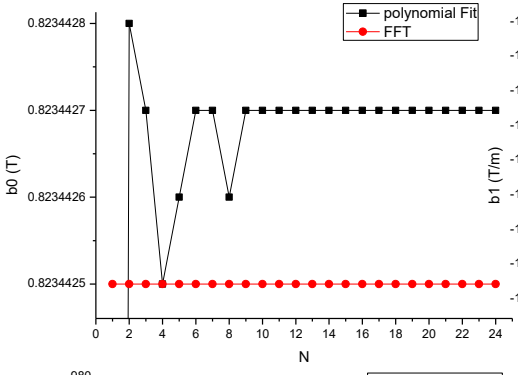

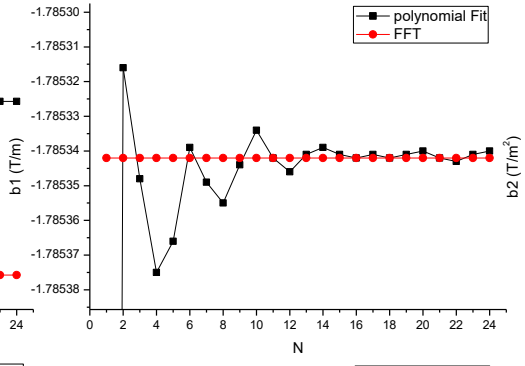

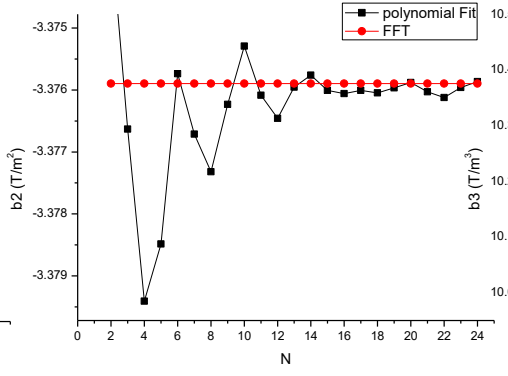

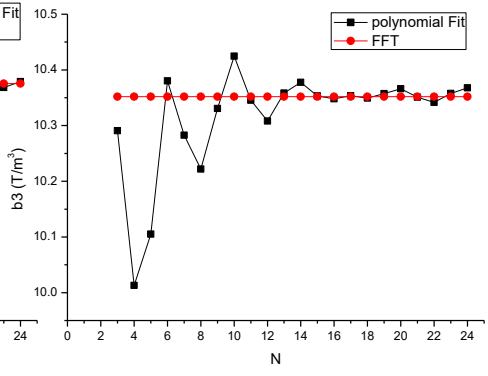

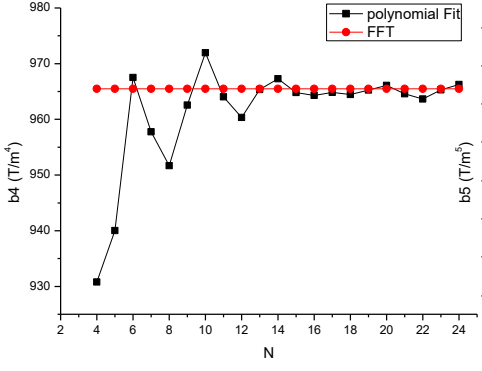

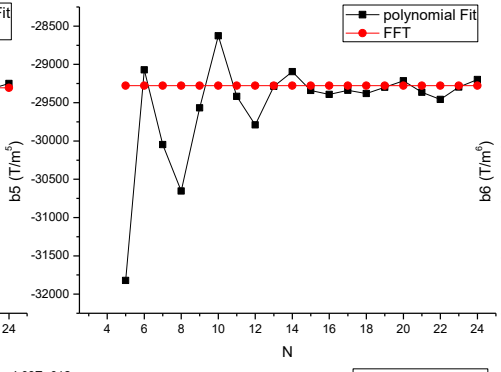

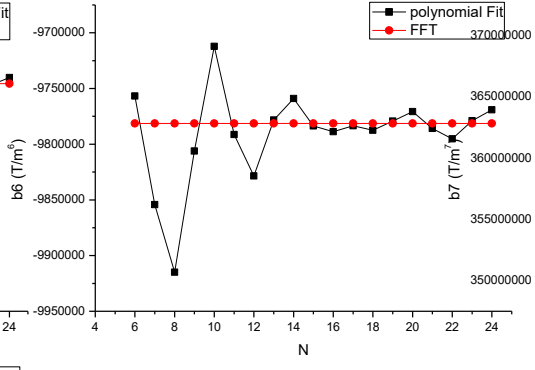

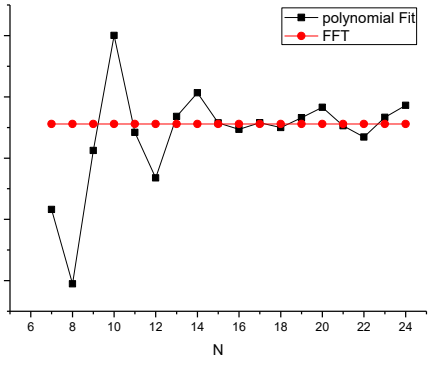

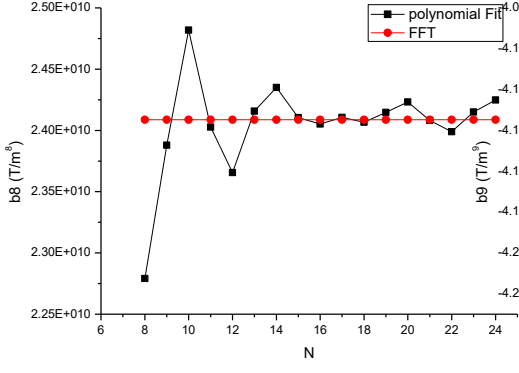

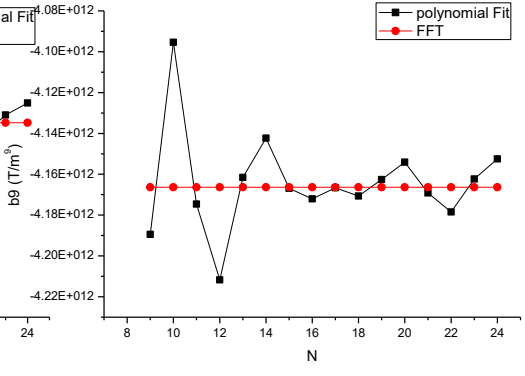

Simulation of a Combined Dipole

Ellipse Ra=20 Rb8 Fitting Number

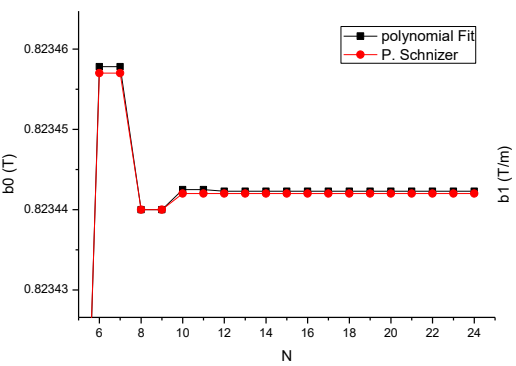

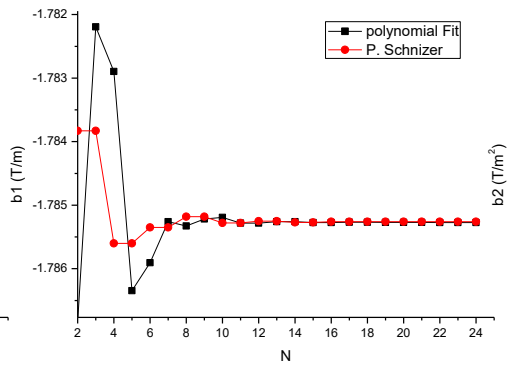

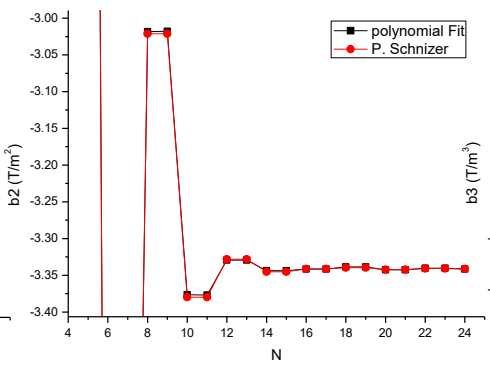

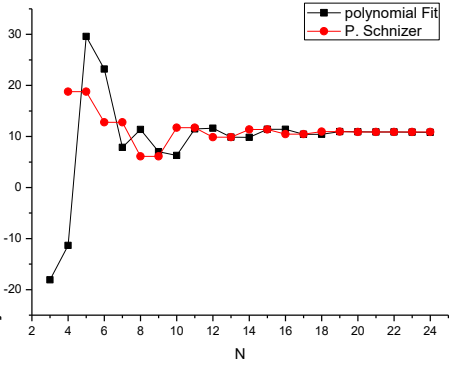

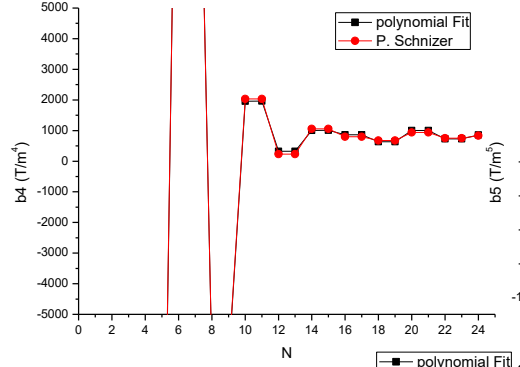

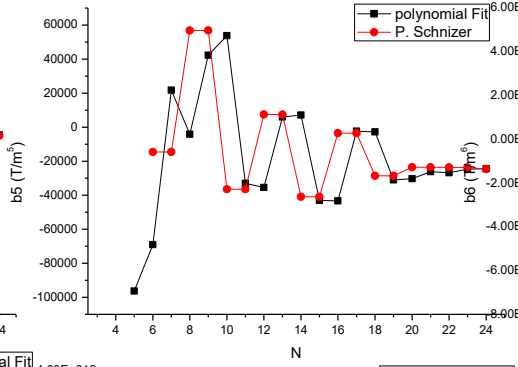

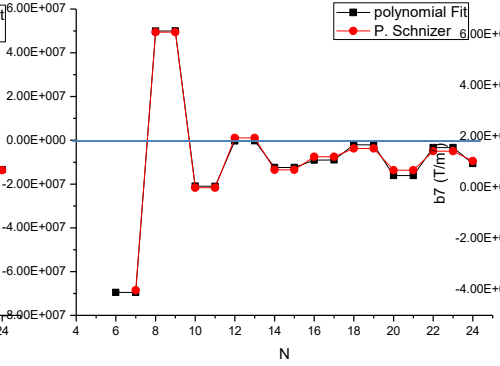

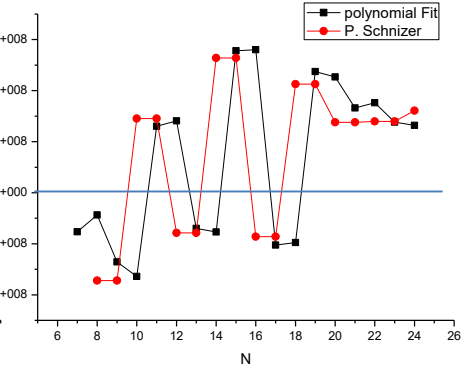

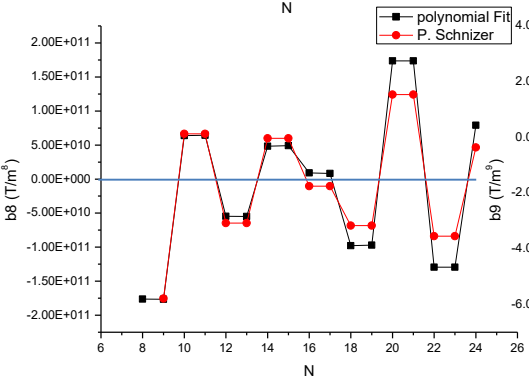

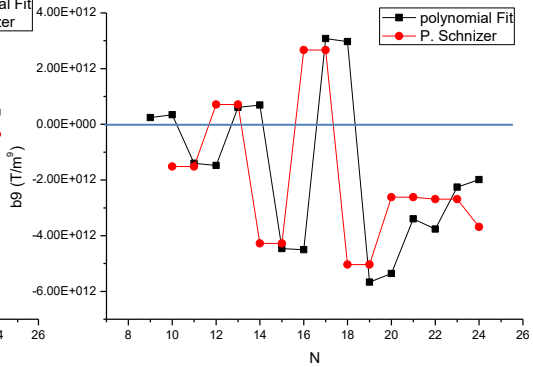

Simulation of a Combined Dipole

Stretched wire measure QM 180A

X(mm)	Mean Iy(G-cm)	STDEV (G-cm)	%	
2182		VR=0.1V		
0	124.9331	2.02206	1.618514	v=25mm/s
5	26095.99	2.7032	0.010359	
10	52052.82	3.89971	0.007492	
15	78037.31	7.30075	0.009355	
20	103991.3	4.60909	0.004432	
25	129934.9	10.92665	0.008409	
30	155890.3	8.40531	0.005392	
35	181813.7	10.61701	0.005839	
2182		VR=0.01V		
0	132.9866	2.36717	1.780006	v=15mm/s
5	26003.88	1.66275	0.006394	
10	51875.94	2.98905	0.005762	
15	77733.24	5.94341	0.007646	
20	103612.1	3.71975	0.00359	
25	129462.5	2.62688	0.002029	
30	155297.1	6.77026	0.00436	
35	OVER			
0	124.5182	2.43309	1.954004	v=25mm/s
5	26061.29	1.88915	0.007249	
10	51998.96	1.92215	0.003697	
15	77928.96	3.39732	0.00436	
20	103863.8	5.58763	0.00538	
25	129772.1	9.35304	0.007207	
30	OVER			

FDI2056	G100			
x	Mean Iy(G-cm)	STDEV (G-cm)	%	
0	134.3428	1.80489	1.343496	v=25mm/s
5	26157.84	1.59773	0.006108	
10	52182.57	4.02849	0.00772	
15	78209.52	4.50289	0.005757	
20	104234.9	3.18839	0.003059	
25	130247.2	2.85603	0.002193	
30	156256.7	2.78412	0.001782	
35	182254.6	5.04362	0.002767	

dx=2mm

Circle vs Ellipse

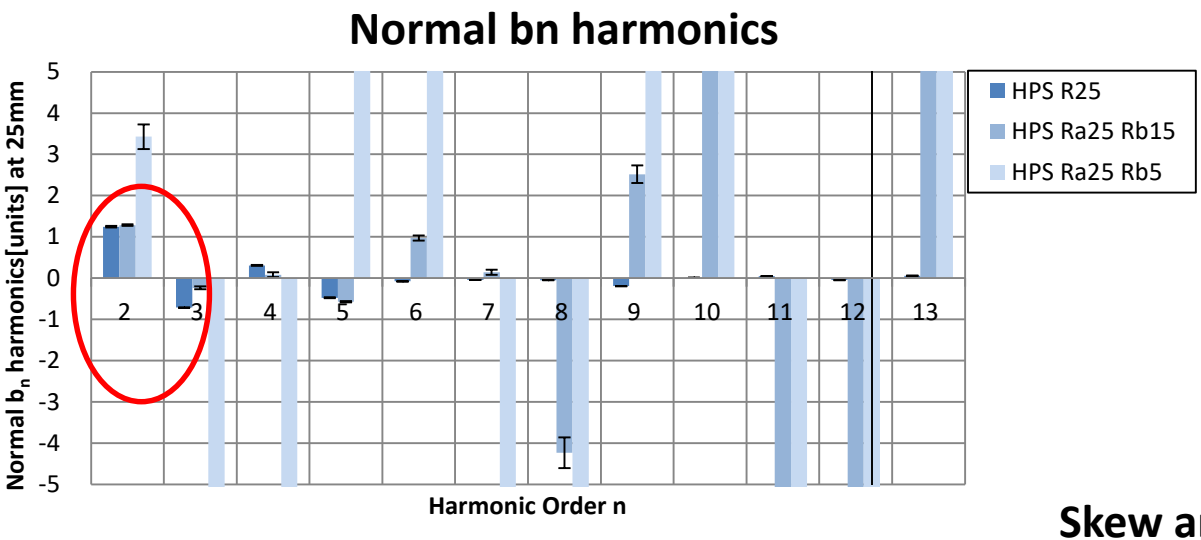

Normalize at long axis radius

HPS Path	B1 (T)
Circle R25	5.178
Ellipse Ra25 Rb15	5.177
Ellipse Ra25 Rb5	5.176

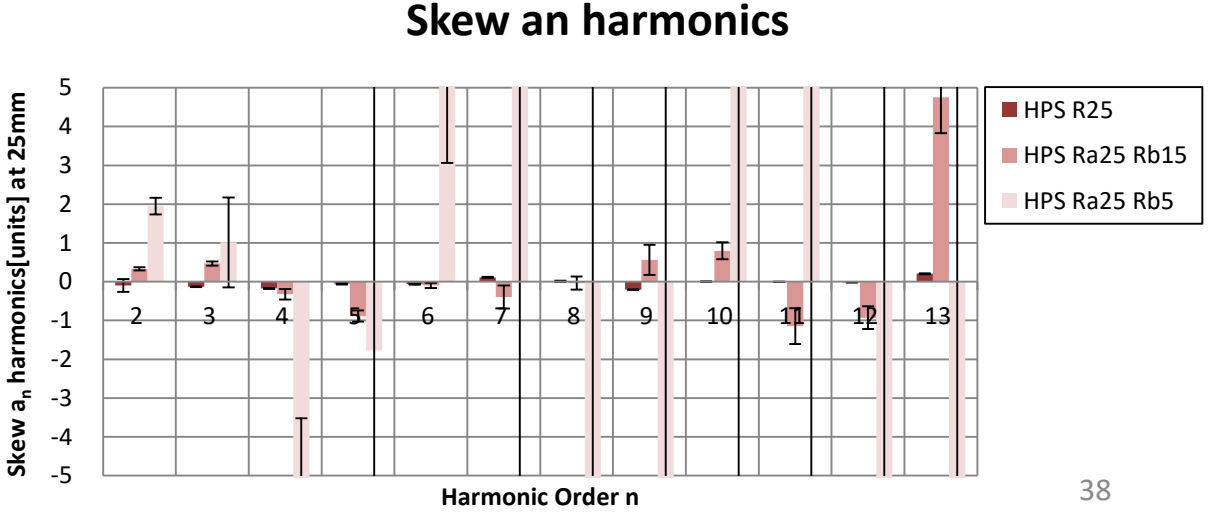

Circle vs Ellipse

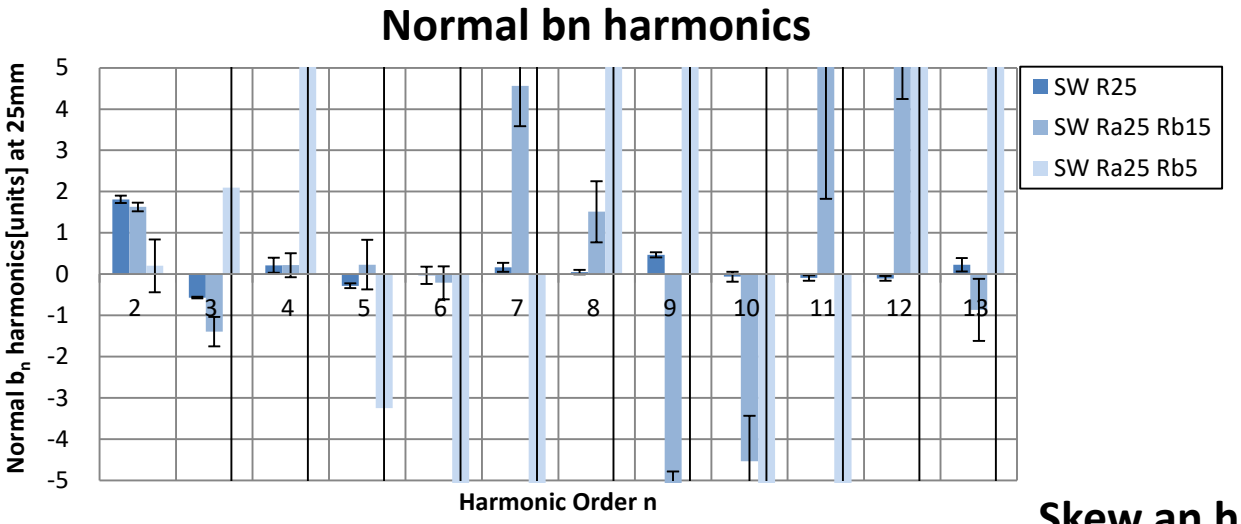

Normalize at long axis radius

SW Path	B1 (T)
Circle R25	5.179
Ellipse Ra25 Rb15	5.174
Ellipse Ra25 Rb5	5.176

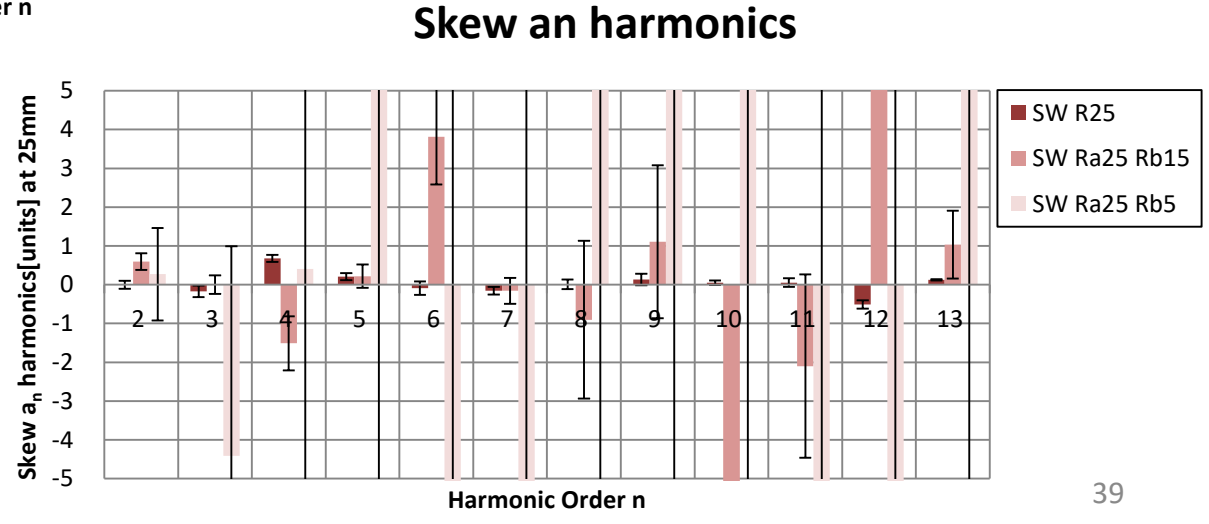

IU24 Gap 7mm

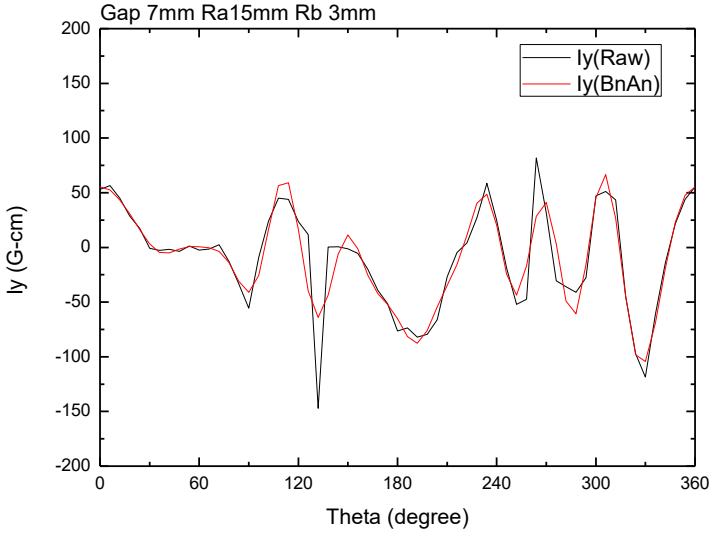

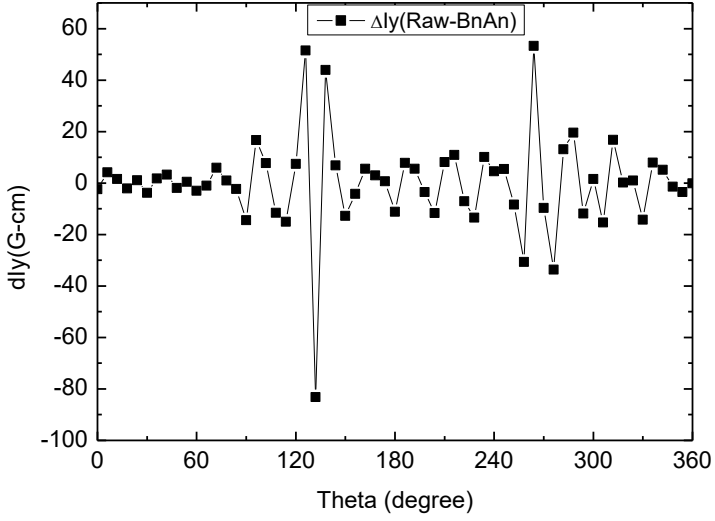

Fit n=12

IU24 Gap 8mm

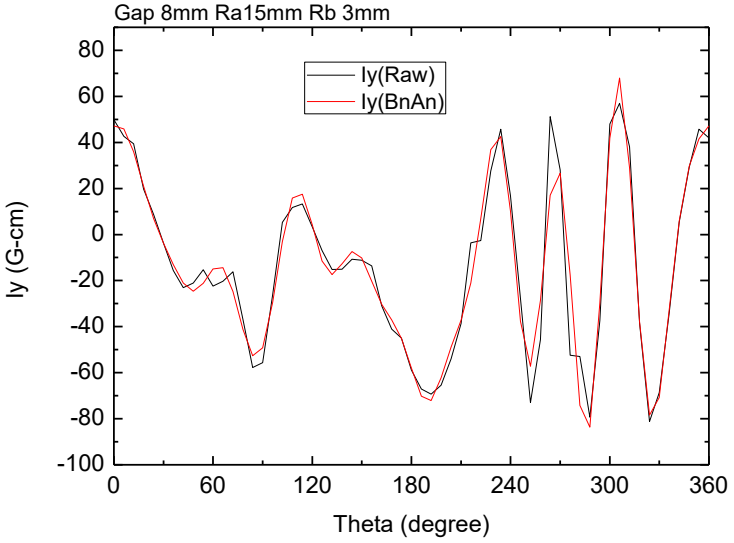

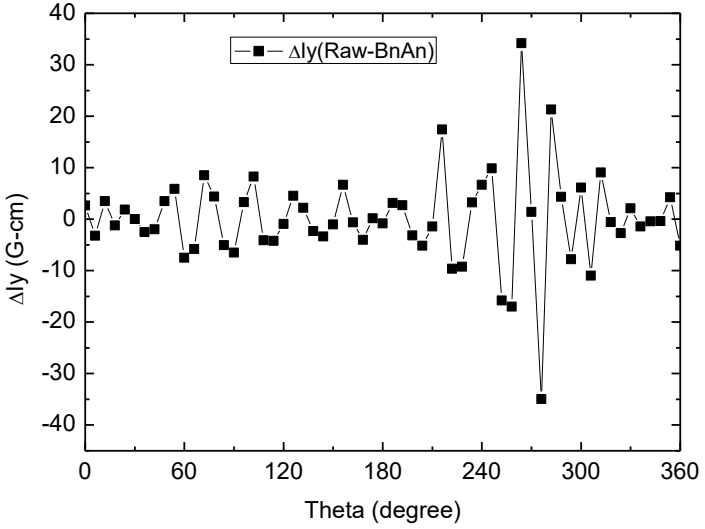

Fit n=12

IU24 Gap 9mm

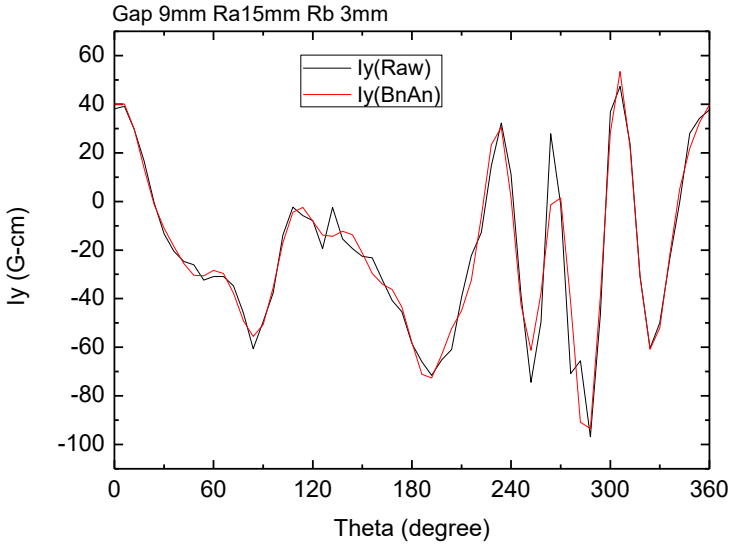

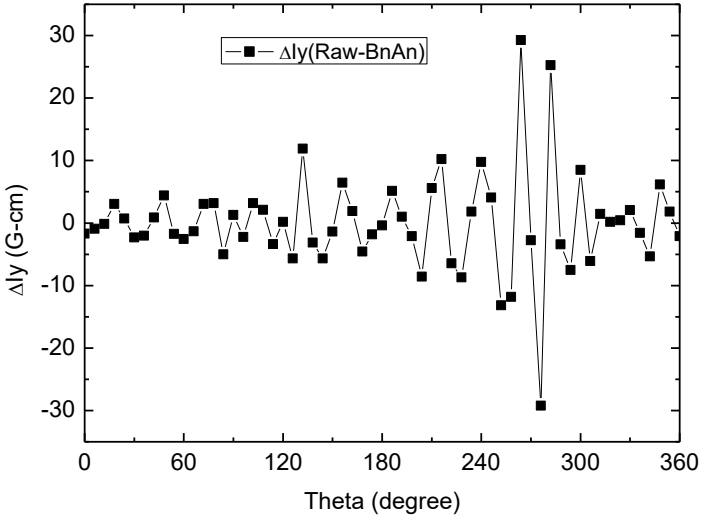

Fit n=12

IU24 Gap 10mm

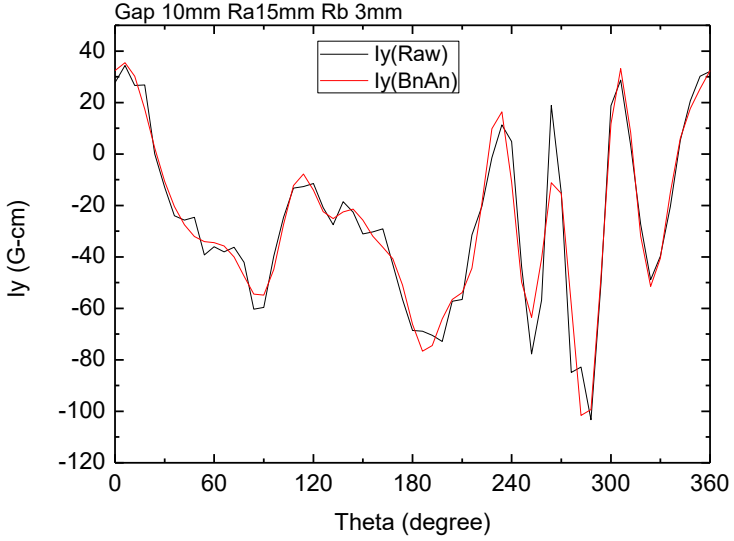

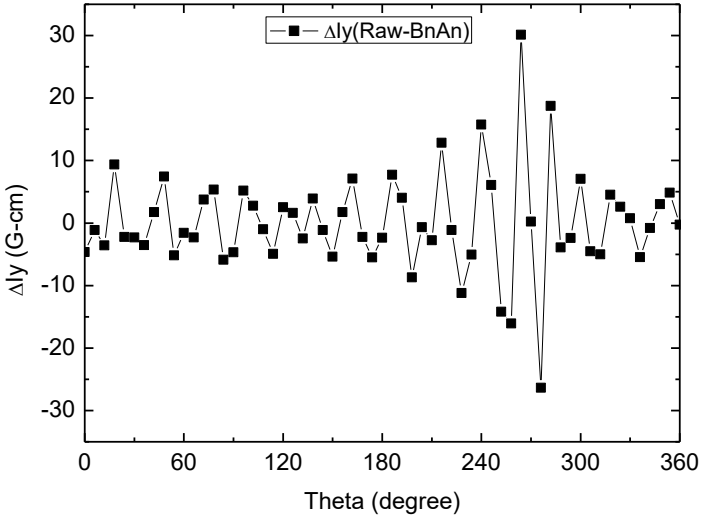

Fit n=12